N-Bound Primary Nitramines Based on 1,5-Diaminotetrazole

Thomas M. Klapötke,* Franz A. Martin, and Jörg Stierstorfer[a]

Abstract: 1,5-Diaminotetrazole can be nitrated under very mild conditions by using nitronium tetrafluoroborate to result in 5-amino-1-nitriminotetrazole (**1**) in good yields. The same reaction can be performed with 1-amino-5-amino-4-methyltetrazole to yield 5-amino-4-methyl-1-nitriminotetrazole (**2**). Both compounds have been isolated and completely characterized by using vibrational spectroscopy, mass spectrometry, and differential scanning calorimetry. Additionally, X-ray diffraction measurements of the neutral compounds could be obtained; they indicated the structure of both compounds to be zwitterionic. Compounds **1** and **2** exhibit extremely high sensitivities to impact and friction and high positive heats of formation of 496 (**1**) and 453 kJ mol^{-1} (**2**), respectively. Additionally, high-nitrogen-containing salts of **1** have been synthesized by metathesis reactions of silver 5-amino-1-nitriminotetrazolate with the corresponding halides so as to investigate the changes in sensitivity and thermal stability. All ionic compounds have been synthesized in good yields and characterized by means of vibrational and multinuclear NMR spectroscopy as well as X-ray diffraction measurements. Thermal stabilities have been evaluated by differential scanning calorimetry, whereas sensitivity measurements have been performed according to standardized Bundesanstalt für Materialforschung und -prüfung (BAM) tests. Theoretical calculations have been performed to investigate the heats of formation as well as the performance characteristics of the compounds.

Keywords: heterocycles · nitramines · nitration · sensitivity · zwitterions

Introduction

The synthesis of new energetic materials has attracted research groups worldwide over the last centuries. Since the discovery of trinitrotoluene (TNT) in 1863 by J. Wilbrand,[1] or pentaerythritol tetranitrate (PETN) in 1894 (Scheme 1),[2] much effort has been put into the development of more powerful, stable, and nontoxic secondary explosives. Hexahydro-1,3,5-trinitro-1,3,4-triazine (RDX) and octahydro-1,3,5,7-tetranitro-1,3,5,7-tetracozine (HMX) (Scheme 1), which were developed between 1920 and 1943,[3] are to this day the most widely used explosive compounds for both civil and military applications. These classic polynitro compounds derive their energy primarily from the oxidation of their carbon backbones by using the nitrogen provided by the nitro substituents.[4] Modern nitro compounds derive their energy not only from the oxidation of their carbon backbone but additionally from ring or cage strain and therefore from their high positive heats of formation. Examples of this new class of compounds are CL-20[5] (Scheme 1)
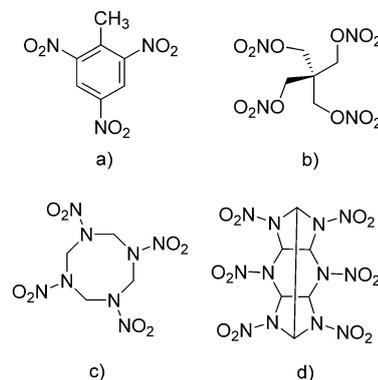
Scheme 1. Classical and modern explosives: a) 1,3,5-trinitrotoluene (TNT), b) pentaerythritol tetranitrate (PETN), c) octogen (HMX), and d) hexanitrahexaazaisowurtzitane (CL-20).

and hepta- or octanitrocubane,[6] which possess very high densities and very good performance characteristics.[7]

Other possibilities for the generation of ring strain and high positive heats of formation are the use of heterocyclic ring systems. five-membered nitrogen-containing heterocycles, 1,2,3,4-tetrazole possesses a high positive heat of formation with $\Delta H_\mathrm{f}^\circ = +237.2$ kJ mol^{-1} relative to 1,2,4-triazole, for example, which provides only $\Delta H_\mathrm{f}^\circ = +109.0$ kJ mol^{-1},[8] These positive heats of formation are achieved due to the high number of N−N and C−N bonds, which yield dinitrogen as the major decomposition product. Notable benefits of these circumstances are the production of more moles of

[a] Prof. Dr. T. M. Klapötke, Dr. F. A. Martin, Dr. J. Stierstorfer
Department of Chemistry
Ludwig-Maximilian-University of Munich
Butenandtstrasse 5–13, Haus D
81377 Munich (Germany)
Fax: (+49)89-2180-77492
E-mail: tmk@cup.uni-muenchen.de

gaseous products per gram of energetic material, along with a higher detonation pressure and the inherently cooler temperature of explosion due to the formation of N_2.[9] Moreover, a good oxygen balance is easier to achieve due to the smaller number of carbon atoms, which leads to the avoidance of environmental pollution as is common for aromatic polynitrocompounds.[10]

The good characteristics of the tetrazole backbone and the "green" approach to energetic materials has made tetrazoles a widely studied system in the research of energetic materials. The formation of 5-nitriminotetrazole, first synthesized in 1949 by O'Connor et al.[11] and further investigated between 1951 and 1953 by Lieber and Herbst,[12] has been utilized as starting material for numerous derivatives: for example, 1- and 2-methyl-5-nitriminotetrazole, or 1- and 2-ethyl-5-nitriminotetrazole.[13] Chemistry with derivatives of 5-nitriminotetrazoles has also been a very large research topic in our group and has resulted in new high-performing secondary explosives as well as pyrotechnical compositions.[3,14] In contrast to this overwhelming collection of compounds, close to no N-bound nitraminotetrazoles are known in the literature. N-Bound nitramines are known for 1,2,4-triazoles and also 1,2,3-triazoles, for example, 4-nitramino-1,2,4-triazole[15] and its alkyl or amine derivatives or 1-nitramino-1,2,3-triazole.[15,16] The same class of compounds is reported for imidazole systems, for example, 1-nitramino-2,5-dinitroimidazole.[17] If we take this variety of N-bound heterocyclic nitramine compounds into consideration, it is surprising that only ammonium and silver salts of 1- and 2-nitriminotetrazole have been described in literature so far, but without providing structural and NMR spectroscopic data.[18] Although theoretical calculations of the neutral 1- and 2-nitriminotetrazole are found in literature,[19] to the best of our knowledge, no neutral N-bound nitriminotetrazole has yet been reported.

Herein we present the first complete study of two novel N-bound nitramines, namely, 5-amino-1-nitrimino-4H-tetrazole and 5-amino-4-methyl-1-nitriminotetrazole based on 1,5-diaminotetrazole. The focus of this study is the full structural as well as spectroscopic characterization of these compounds and the formation and complete characterization of high-nitrogen-containing salts of 5-amino-1-nitrimino-4H-tetrazole using ammonium, hydrazinium, guanidinium, aminoguanidinium, and triaminoguanidinium as counterions. The potential application of the synthesized compounds as energetic materials will be studied and evaluated using the experimentally obtained values for thermal decomposition as well as sensitivity data together with calculated performance characteristics.

Results and Discussion

Synthesis: 1,5-Diaminotetrazole (DAT) was synthesized according to the literature by the reaction of thiosemicarbazide with two equivalents of sodium azide, ammonium chloride, and lead(II) oxide each.[20] The methylated derivative,

1,5-diamino-4-methyltetrazole (MeDAT), was synthesized according to the literature, starting with the methylation of DAT with six equivalents of methyl iodide in acetonitrile to form 1,5-diamino-4-methyltetrazolium iodide selectively, followed by deprotonation with potassium hydroxide in methanol and subsequent sublimation to obtain pure MeDAT.[21]

The nitration of DAT and MeDAT to form 5-amino-1-nitrimino-4H-tetrazole (**1**) and 5-amino-4-methyl-1-nitriminotetrazole (**2**) was performed by using one equivalent of nitronium tetrafluoroborate in dry acetonitrile at 0°C (Scheme 2).
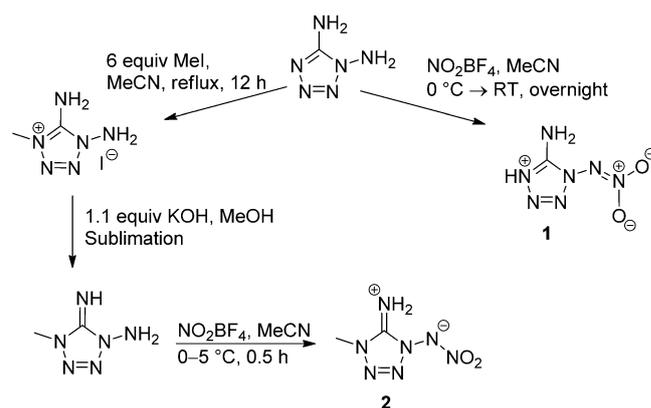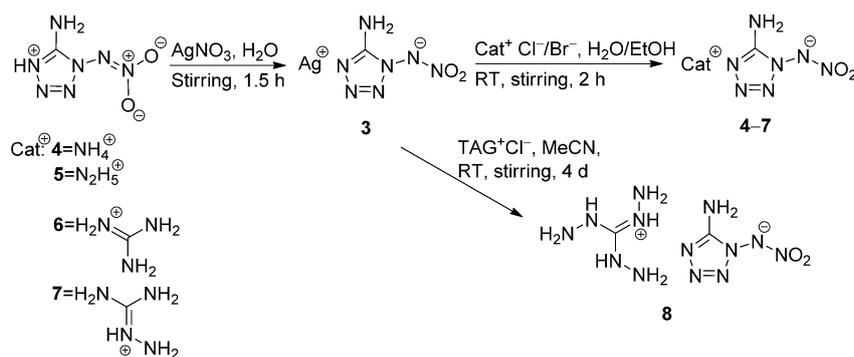

Scheme 2. Reaction pathway towards the formation of 5-amino-1-nitrimino-4H-tetrazole (**1**) and 5-amino-4-methyl-1-nitriminotetrazole (**2**).

Even though attempts were undertaken to eliminate the very expensive nitration reagent nitronium tetrafluoroborate, none of these attempts resulted in reasonable yields, often not even of the desired compound. Compound **1** was obtained in only 3% yield by usage of a nitration mixture that consisted of concentrated sulfuric acid and 100% nitric acid in a 3:1 ratio after various attempts. The mixture was extracted with diethyl ether immediately after quenching with ice water, otherwise **1** was destroyed by acidic hydrolysis. The different reaction routes are summarized in Scheme 3.
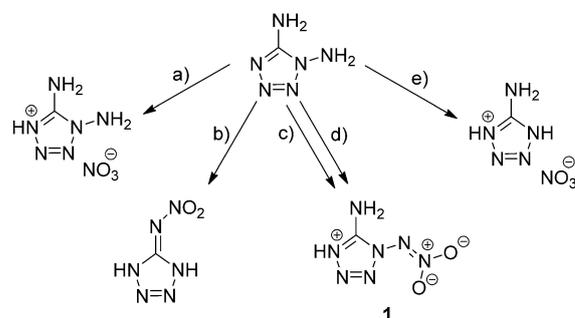
Scheme 3. Reaction routes using different nitration reagents starting from 1,5-diaminotetrazole. Conditions: a) 65% HNO_3 or N_2O_5 1 equiv, MeCN; b) 100% HNO_3/Ac_2O; c) ratio 1:3, 100% HNO_3/H_2SO_4, 0°C, yield: 3%; d) NO_2BF_4, MeCN, 0°C, yield: 55%; e) N_2O_5 (excess), MeCN.

Scheme 4. Reaction pathways by means of the metathesis reaction of silver 5-amino-1-nitriminotetrazolate (**3**) with nitrogen-rich cations.

The formation of the nitrogen-rich salts was accomplished in a straightforward manner by metathesis reactions that used silver 5-amino-1-nitriminotetrazolate (**3**) with the corresponding halides in water/ethanol mixtures (**4–7**) or acetonitrile in the case of the triaminoguanidinium salt (**8**). Compound **3** was synthesized by the addition of a small excess of silver nitrate to a solution of **1** in water. The reaction pathways are presented in Scheme 4. Since **2** has a very high decomposition temperature (150 °C) for a neutral nitraminotetrazole, the corresponding salts should exhibit an even higher thermal stability together with a decrease in sensitivity when compared with the high-nitrogen-containing salts of **1**. However, all attempts to deprotonate **2** failed; compound **2** was always recovered as the neutral compound. The same reason for the high thermal stability of **2** also prohibits the compound from donating a proton to guanidine bases. Compound **2** is a zwitterionic compound, with the amine group carrying the positive charge, whereas the negative charge is located on the nitrimine and gains its high stability from this circumstance together with the $+I$ inductive effect of the methyl group that donates electron density to the tetrazole ring. Compound **1** is also a zwitterionic compound, but the hydrogen atom on the 4-position is too acidic to stabilize the system and is therefore easily donated to bases.

Molecular structures: Single-crystal X-ray diffraction studies have been undertaken for compounds **1**, **2**, and **4–8**. Whereas **1** has been recrystallized from diethyl ether to yield colorless blocks, compounds **2** and **8** have been recrystallized from acetonitrile as colorless plates and rods, respectively. The nitrogen-rich salts **4–7** have been recrystallized without crystal water from ethanolic solutions by using an ethanol/water ratio of 9:1. Selected crystallographic data for all compounds have been compiled in Table S1 in the Supporting Information. A discussion of the structural parameters of all compounds with respect to the DATNO$_2$ moieties is performed first; the effects of methylation and deprotonation on the DATNO$_2$ moiety are evaluated. A compilation of selected bond lengths, bond angles, and torsion angles of compounds **1**, **2**, and **4–8** is presented in Table 1. Additionally,

the structures of the two neutral compounds, 5-amino-1-nitrimino-4H-tetrazole (**1**) and 5-amino-4-methyl-1-nitriminotetrazole (**2**), are discussed in detail. Since all ionic structures are composed of strong hydrogen-bonded networks, only one compound, the ammonium 5-amino-1-nitriminotetrazolate (**4**), which presents the most interesting structure, is discussed as an example. The hydrogen bonds present in compounds **5–8**, which are not discussed in detail, are compiled in Tables S2–S5 in the Supporting Information. Since all ionic structures exhibit nearly the same structure, the asymmetric units of **5–7** are shown in Figures S1–S3 in the Supporting Information, and only **4** and **8** are presented as examples in the discussion.

The discussion of the structure displayed by the guanidinium cations is completely omitted because they do not differ by much from the already performed studies that are known from the literature.[22] As observed for tetrazoles in general, the bond lengths of the C–N and N–N bonds within the tetrazole moiety of **1** are located between the lengths of formal single and double bonds (C–N: 1.47, 1.22 Å; N–N: 1.48, 1.20 Å),[23] which indicate the aromatic character of the compounds. The N–N bonds show distances between 1.279(3) (N2–N3) and 1.370(3) Å, whereas the two C–N bonds show distances of 1.333(3) (C1–N4) and 1.346(3) Å (C1–N1). The amine group in the 5-position shows a bond length towards the tetrazole ring of only 1.311(3) Å and is hence closer to a formal double bond, thereby resulting in an sp^2-hybridized nitrogen atom N7, which forces the amine group into a nearly planar geometry setting. The bond is shortened by 0.03 Å relative to the educt (DAT, 1.3422(3) Å). The positive charge must therefore be distributed between N4 and N7, whereas the negative charge is more narrowly located on the N5 bridging atom of the nitramine group. The N1–N5 bond is longer than the N5–N6 bond, which display 1.383(3) and 1.353(3) Å, respectively. Both bonds are in between formal single and double bonds, and together with the short N–O distances of the nitro group (1.229(3) (N6–O1) and 1.244(2) Å (N6–O2)), present a delocalized π-electron system with partial charges located on O1 and O2 (negative) and on the N6 atom (positive). The zwitterionic character of the compound is obvious, since the hydrogen atom H4 is located on the ring atom site, not on the nitramine substituent, as far apart as possible.

Only very small deviations are observed for the molecular structure of **2**, which basically displays the same pattern as observed for **1**. The C1–N7 bond (1.302(2) Å) is shortened by 0.01 Å compared to **1**. This is even closer to a formal double bond (1.22 Å), which again results in the planar geometry of the amine group N7. The same distribution of the

Table 1. Selected bond lengths [Å], bond angles [°], and torsion angles [°] that indicate the geometries of the DATNO$_2$ moieties.

	HDATNO$_2$ (1)	NH$_4^+$, 1st (4)	NH$_4^+$, 2nd (4)	N$_2$H$_5^+$ (5)	G$^+$ (6)	AG$^+$ (7)	TAG$^+$ (8)	MeDATNO$_2$ (2)
N1−N2	1.370(3)	1.364(2)	1.367(2)	1.364(2)	1.360(3)	1.371(2)	1.361(3)	1.365(2)
N2−N3	1.279(3)	1.279(2)	1.290(2)	1.284(2)	1.287(3)	1.290(2)	1.299(3)	1.273(2)
N3−N4	1.362(3)	1.362(2)	1.373(2)	1.369(2)	1.361(3)	1.372(2)	1.370(3)	1.371(2)
N4−C1	1.333(3)	1.329(2)	1.333(2)	1.327(2)	1.336(3)	1.321(2)	1.325(3)	1.332(2)
C1−N1	1.346(3)	1.345(2)	1.351(2)	1.346(2)	1.341(3)	1.347(2)	1.346(3)	1.341(2)
N1−N5	1.383(3)	1.392(2)	1.400(2)	1.386(2)	1.391(3)	1.393(2)	1.401(3)	1.390(2)
N5−N6	1.352(3)	1.340(2)	1.323(2)	1.333(2)	1.335(3)	1.328(2)	1.318(3)	1.336(2)
N6−O1	1.229(3)	1.248(1)	1.249(2)	1.246(2)	1.242(3)	1.250(2)	1.261(3)	1.227(2)
N6−O2	1.244(2)	1.249(1)	1.260(2)	1.259(2)	1.252(2)	1.258(2)	1.257(2)	1.258(2)
C1−N7	1.311(3)	1.340(2)	1.333(2)	1.336(2)	1.327(3)	1.342(2)	1.344(4)	1.302(2)
N7−H7a	0.89(3)	0.92(2)	0.81(2)	0.95(2)	0.94(3)	0.85(2)	0.85(3)	0.87(2)
N7−H7b	0.82(3)	0.88(2)	0.84(2)	0.87(2)	0.84(3)	0.92(2)	0.86(2)	0.90(2)
N4−H1 (CH$_3$)	0.96(3)	−		−	−	−	−	1.448(2)
N1-N2-N3	107.1(2)	105.6(1)	105.6(1)	105.5(1)	105.1(2)	105.3(1)	105.6(2)	107.7(1)
N2-N3-N4	108.7(2)	112.2(1)	112.0(1)	112.0(1)	112.4(2)	111.9(1)	111.0(2)	108.2(1)
N3-N4-C1	109.7(2)	105.5(1)	105.5(1)	105.6(1)	105.2(2)	105.6(1)	106.4(2)	109.7(1)
N4-C1-N1	104.6(2)	107.9(1)	108.0(1)	107.9(2)	107.7(2)	108.4(2)	107.6(2)	104.6(1)
C1-N1-N2	109.8(2)	108.9(1)	109.0(1)	109.0(2)	109.5(2)	108.8(1)	109.4(2)	110.0(1)
N1-C1-N7	126.5(2)	124.9(1)	124.5(1)	123.7(2)	124.1(2)	122.8(2)	124.0(2)	126.2(2)
C1-N1-N5	127.0(2)	130.6(1)	121.8(1)	127.2(2)	126.7(2)	125.1(1)	129.9(2)	126.0(1)
N1-N5-N6	109.4(2)	109.4(1)	111.5(1)	109.8(2)	109.9(2)	110.0(1)	110.0(2)	108.7(1)
N5-N6-O1	122.6(2)	123.1(1)	123.3(1)	124.3(1)	124.4(2)	123.2(1)	123.8(2)	124.1(1)
N5-N6-O2	114.3(2)	115.2(1)	115.3(1)	115.1(1)	114.7(2)	115.6(1)	115.5(2)	113.3(1)
O1-N6-O2	123.1(2)	121.7(1)	121.3(1)	120.6(2)	120.9(2)	121.2(2)	120.7(2)	122.5(1)
N2-N1-N5-N6	97.5(2)	−109.2(1)	69.3(2)	91.3(2)	−89.8(3)	−80.3(2)	−114.2(2)	98.0(2)
N1-N5-N6-O1	−1.6(3)	−2.7(2)	−10.2(2)	−1.0(2)	−1.1(3)	−0.7(2)	−2.1(3)	−0.5(2)

partial charges can be stated for **2** relative to **1**. Even though a positive charge is located on the amine group, no deprotonation was possible at this position, thus indicating a very stable zwitterionic configuration; this is also aided by the +I effect of the methyl group in the 4-position, which donates electron density to the heterocyclic ring system. The bond and torsion angles are basically the same for **1** and **2** with only slight deviations of <1.5°. Even the nitramine moiety is twisted out of the tetrazole plane at nearly the same value (97.5(2)° (**1**), 98.0(2)° (**2**)).

The bond lengths differ only slightly for the anion of **1** in compounds **4–8**. The N4−H4 bond is missing due to deprotonation, hence the C1−N7 bond is elongated for all ionic compounds between +0.016 (**6**) and +0.033 Å (**8**) and the positive partial charge is diminished slightly. The second difference is observed for the N1−N5 and N5−N6 bonds. Whereas the N1−N5 bond is elongated slightly (mean value: 0.011 Å), the N5−N6 bond is shortened much more (mean value: 0.23 Å), yet the two N−O bonds of the nitro group are elongated at the same time. The elongations are in the range between 0.011 (N6−O2, mean value) and 0.20 Å (N6−O1, mean value).

The biggest difference between **1** and the anions presented in **4–8** are the bond angles within the tetrazole moieties, which differ up to 3.7°. The deprotonation at the 4-position changes all three bond angles in which the N4 atom participates: N2-N3-N4, N3-N4-C1, and N4-C1-N1. Whereas N2-N3-N4 and N4-C1-N1 are both widened by 3.2 and 3.3° (mean values), respectively, N3-N4-C1 is reduced by −4.0°

(mean value, Table 1). The O-N-O angle at the nitro group is also reduced and approaches the standard bond angle of 120° for the planar geometry of the nitro group. The N2-N1-N5-N6 torsion angle varies widely and shows angles between −114.2 and +91.3° forced by the packing scheme within the crystal structures aided by free rotation around the N1−N5 bond.

5-Amino-1-nitrimino-4H-tetrazole (**1**) crystallizes in the orthorhombic space group $Pna2_1$ with a cell volume of 525.03(4) Å^3 and four molecular moieties in the unit cell. The calculated density at 200 K is 1.835 g cm^{-3} and hence in the range of other nitriminotetrazoles, for example, 5-nitramino-1H-tetrazole at 1.867 g cm^{-3}.[14d] The asymmetric unit of **1** together with the atom-labeling scheme is presented in Figure 1.
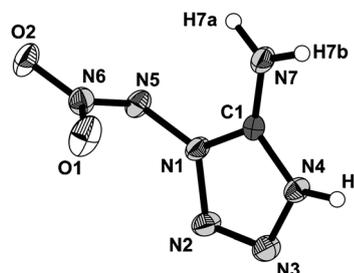

Figure 1. Asymmetric unit of **1**. Thermal ellipsoids are set to 50% probability.

The crystal structure of **1** is built up by six hydrogen bonds (Figure 2, Table 2), which use only the amine group and the N4 hydrogen as donor atoms. All three donor sites
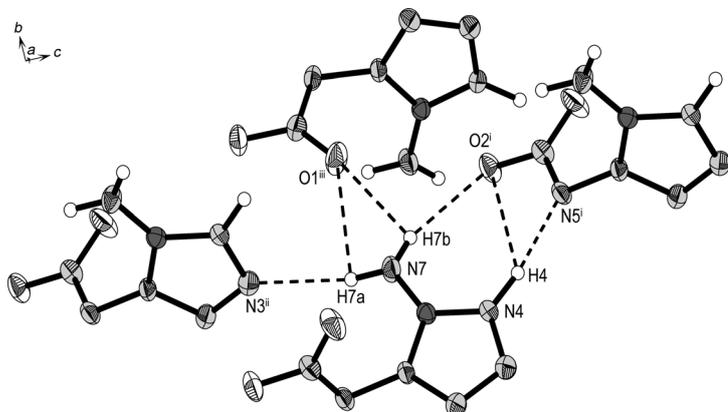

Figure 2. Hydrogen-bonding scheme in the structure of **1** displayed for the asymmetric unit only for reasons of clarity. Thermal ellipsoids are set to 50% probability. Symmetry operators: i) $-x+\frac{1}{2}$, $y+\frac{1}{2}$, $z+\frac{1}{2}$; ii) $-x+\frac{1}{2}$, $y+\frac{1}{2}$, $z-\frac{1}{2}$; iii) $x+\frac{1}{2}$, $-y+\frac{5}{2}$, z.

Table 2. Hydrogen bonds present in **1**.[a]

D−H···A	d(D−H) [Å]	d(H···A) [Å]	d(D−H···A) [Å]	$<$(D−H···A) [°]
N4−H4···N5[i]	0.96(3)	1.80(3)	2.760(2)	171(2)
N4−H4···O2[i]	0.96(3)	2.67(2)	3.278(2)	121(2)
N7−H7a···N3[ii]	0.89(3)	2.15(3)	3.019(3)	166(2)
N7-H7a···O1[iii]	0.89(3)	2.67(3)	2.826(3)	91(2)
N7−H7b···O2[i]	0.82(3)	2.20(3)	2.968(3)	157(3)
N7−H7b···O1[iii]	0.82(3)	2.42(3)	2.826(3)	111(2)

[a] Symmetry operators: i) $-x+\frac{1}{2}$, $y+\frac{1}{2}$, $z+\frac{1}{2}$; ii) $-x+\frac{1}{2}$, $y+\frac{1}{2}$, $z-\frac{1}{2}$; iii) $x+\frac{1}{2}$, $-y+\frac{5}{2}$, z.

N4−H4, N7−H7a, and N7−H7b form bifurcated hydrogen bonds. Three hydrogen bonds can be considered moderately strong hydrogen bonds, with H···A distances of 1.80(3), 2.15(3), and 2.20(3) Å, respectively, for N4−H4···N5(i), N7−H7a···N3(ii), and N7−H7b···O2(i). They are also not only of electrostatic nature but directed with D−H···A angles of 171(2), 166(2), and 157(3)°, respectively. The other three hydrogen bonds, which always represent the second hydrogen bond formed by the donor atoms N4−H4···O2(i), N7−H7a···O1(iii), and N7−H7b···O1(iii) are much weaker with H···A distances of 2.67(2), 2.42(3), and 2.67(3) Å, respectively. They are mostly of electrostatic nature with D−H···A angles of only 121(2), 111(2), and 91(2)°.

The hydrogen bonds discussed build up a very dense 3D network as shown in Figure 3. The 3D network consists of condensed "rhombic prisms" built by the HDATNO₂ molecules with an enclosed angle of 67.44°. The prisms of HDATNO₂ molecules are stacked along the *c* axis, whereas the representation in Figure 3 displays a view coplanar to the *ab* plane. The formation of these structures is aided by the torsion angle between the tetrazole ring and the nitramine group.
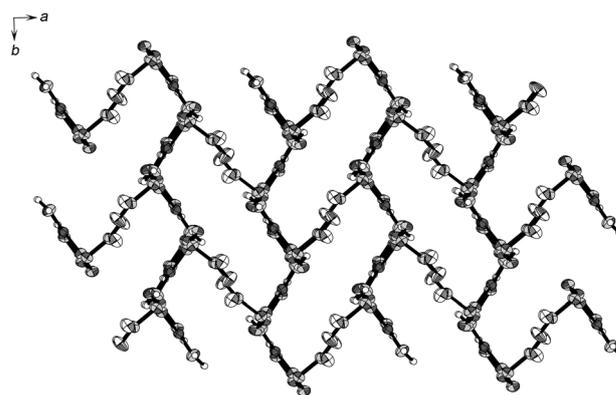

Figure 3. Packing scheme of the crystal structure along the *c* axis in **1** displayed coplanar to the *ab* plane. Thermal ellipsoids are set to 50% probability.

5-Amino-4-methyl-1-nitriminotetrazole (**2**) crystallizes in the monoclinic space group $P2_1/n$ with a cell volume of 643.2(2) Å³ and four molecular moieties in the unit cell. The calculated density at 173 K is 1.643 g cm⁻³ and hence 0.1 g cm⁻³ lower than 1-methyl-5-nitramino-1*H*-tetrazole, which has a density of 1.755 g cm⁻³.[14d] The asymmetric unit of **2** together with the atom labels is presented in Figure 4.
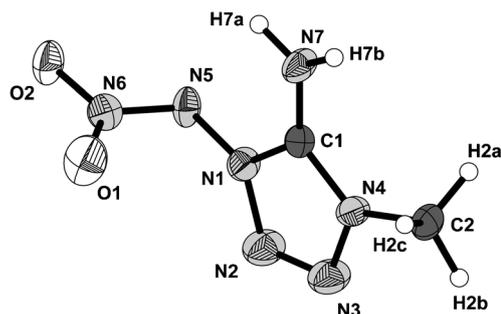

Figure 4. Asymmetric unit of **2**. Thermal ellipsoids are set to 50% probability.

The crystal structure of **3** is built up by mainly three hydrogen bonds (Figure 5). Only the N7−H7a···O2(ii) hydrogen bond is of electrostatic nature and rather weak with an H···A distance of 2.63(2) Å; it is the second bond from a bifurcated hydrogen-bonding scheme with N7 as the donor atom. The D···A distances of the other two hydrogen bonds, N7−H7a···N5(ii) and N7−H7b···O2(i) are significantly below the sum of van der Waals radii at 2.935(2) and 2.815(2) Å, respectively (r_w(N)+r_w(N) = 3.10 Å; r_w(N)+r_w(O) = 3.07 Å).[23] These hydrogen bonds build up a planar, either twelve- or eight-membered ring system, depending on the bifurcated hydrogen bonds under consideration. This ring motif connects four MeDATNO₂ molecules, each of which lie opposite to one another. Due to the different positions of the nitramine moiety, this pattern is repeated, always twisted by the torsion angle of the nitramine group toward the tetrazole ring (98.0°), and therefore an extended 3D net-

Figure 5. Hydrogen-bonding pattern within the structure of **3** displaying the motif for the formation of a 3D network. Thermal ellipsoids are set at 50% probability. Symmetry operators: i) $x+\frac{1}{2}$, $-y-\frac{1}{2}$, $z+\frac{1}{2}$; ii) $-x+\frac{1}{2}$, $y-\frac{1}{2}$, $-z+\frac{1}{2}$; iii) $-x+\frac{3}{2}$, $y+\frac{1}{2}$, $-z+\frac{1}{2}$.

Figure 6. Asymmetric unit of **4**. Thermal ellipsoids are set to 50% probability.

work is formed. The presentation of the unit cell is omitted because it does not offer additional information. The fourth hydrogen bond connects the methyl group to the O1(iii) atom of the nitro group over C2−H2b. The hydrogen bond is moderately strong; it has a D···A distance of 3.159(2) Å, which is shorter than the sum of van der Waals radii $(r_w(C)+r_w(O)=3.21$ Å).[23]

Ammonium 5-amino-1-nitriminotetrazolate (**4**) crystallizes in the monoclinic space group $C2/c$ with a cell volume of 2451.1(2) Å³ and 16 molecular moieties in the unit cell. The calculated density at 173 K is 1.757 g cm⁻³. The asymmetric unit of **4** (Table 3), which consists of two independent ammonium 5-amino-1-nitriminotetrazolate moieties, together with atom labels is presented in Figure 6.

Table 3. Hydrogen bonds present in **2**.[a] The C−H hydrogen atom of the methyl group is set restrained, therefore no standard deviations are given.

D−H···A	d(D−H) [Å]	d(H···A) [Å]	d(D−H···A) [Å]	$<$(D−H···A) [°]
N7−H7b···O2^i	0.87(2)	1.99(2)	2.815(2)	157.9(16)
N7−H7a···N5^{ii}	0.90(2)	2.04(2)	2.935(2)	170.5(18)
N7−H7a···O2^{ii}	0.90(2)	2.63(2)	3.141(2)	117.0(15)
C2−H2b···O1^{iii}	0.98	2.37	3.159(2)	137

[a] Symmetry operators: i) $x+\frac{1}{2}$, $-y-\frac{1}{2}$, $z+\frac{1}{2}$; ii) $-x+\frac{1}{2}$, $y-\frac{1}{2}$, $-z+\frac{1}{2}$; iii) $-x+\frac{3}{2}$, $y+\frac{1}{2}$, $-z+\frac{1}{2}$.

All hydrogen bonds observed in the structure of **4** can be considered moderately strong with D···A distances all below or within the standard deviations of the sum of van der Waals radii (Table 4). Hydrogen bonds that show strong, mostly electrostatic interactions are formed only with oxygen atoms as acceptor molecules (N7a−H7aa···O2, N8−H8a···O1(iii), and N8−H8b···O2 with D−H···A angles of 139(2), 128(2), and 114(2)°). Since the asymmetric unit of **4** consists of two independent sets of cations and anions, two

Table 4. Hydrogen bonds present in **4**.[a]

D−H···A	d(D−H) [Å]	d(H···A) [Å]	d(D−H···A) [Å]	$<$(D−H···A) [°]
N7−N7a···O2a	0.92(2)	2.12(2)	3.030(2)	167(1)
N7−H7b···O2^i	0.88(2)	2.16(2)	3.002(2)	161(2)
N7a−H7ab···O1a^{ii}	0.84(2)	2.10(2)	2.919(2)	165(2)
N7a−H7aa···O1	0.81(2)	2.27(2)	3.057(2)	166(2)
N7a−H7aa···O2	0.81(2)	2.56(2)	3.213(2)	139(2)
N8−H8a···O1^{iii}	0.83(2)	2.24(2)	2.832(2)	128(1)
N8−H8a···N2^{iv}	0.83(2)	2.38(2)	3.003(2)	132(1)
N8−H8b···N5	0.96(2)	2.00(2)	2.941(2)	166(1)
N8−H8b···O2	0.96(2)	2.61(2)	3.128(2)	114(1)
N8−H8c···N4^v	0.97(2)	1.95(2)	2.915(2)	174(1)
N8−H8c···N3^v	0.97(2)	2.62(2)	3.447(2)	144(1)
N8−H8d···N3a^{vi}	0.94(2)	2.11(2)	3.053(2)	178(1)
N8a−H8ad···N4a^{vii}	0.95(2)	1.94(2)	2.888(2)	171(1)
N8a−H8ac···N3^{viii}	0.90(2)	2.10(2)	2.975(2)	166(2)
N8a−H8ab···N5a^{ix}	0.93(2)	2.21(2)	3.103(2)	161(1)
N8a−H8aa···N2a^{vi}	0.87(2)	2.49(2)	3.161(2)	135(1)

[a] Symmetry operators: i) x, $y-1$, z; ii) x, $-y+1$, $z-\frac{1}{2}$; iii) x, $-y+1$, $z+\frac{1}{2}$; iv) $-x$, y, $-z+\frac{1}{2}$; v) $-x$, $y+1$, $-z+\frac{1}{2}$; vi) $-x+\frac{1}{2}$, $y+\frac{1}{2}$, $-z+\frac{1}{2}$; vii) $-x+\frac{1}{2}$, $-y+\frac{3}{2}$, $-z$; viii) $-x$, $-y+1$, $-z$; ix) x, $y+1$, z.

sets of hydrogen bonds are formed for each pair; the sets are connected over two hydrogen bonds, N8−H8d···N3a(vi) and N8a−H8aa···N2a(vi). The hydrogen-bonding motifs for the surrounding of each ammonium ion are presented in Figure 7.

If one takes a look at the connection between the DATNO₂⁻ anions themselves, two independent sets of rows can be identified (Figure 8). One row consists of the first independent set of DATNO₂⁻ anions connected by the N7−H7b···O2(i) hydrogen bond, whereas the second row, which lies nearly perpendicular to the first one and encloses an angle of 86.02° in between, is formed by the second set of DATNO₂⁻ anions connected by N7a−H7ab···O1a(ii). The rows are connected to one another by three hydrogen bonds, N7H7a···O2a, N7a−H7aa···O1, and N7a−H7aa···O2. Hence the rows lie always coplanar to one another, whereas the ammonium cations build connections between the rows.
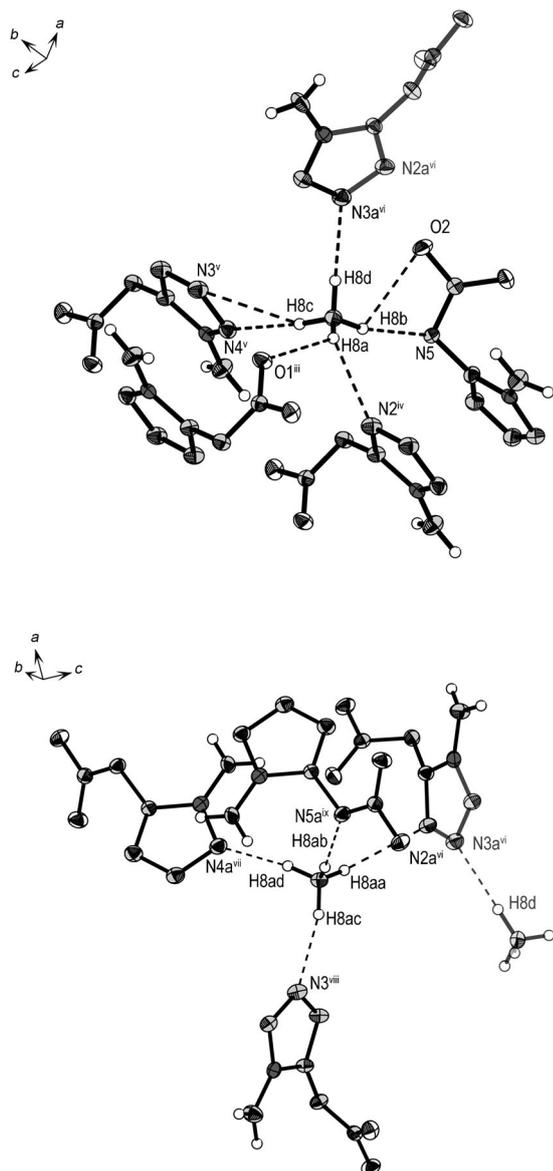
Figure 7. Surroundings of the two independent ammonium cations formed by hydrogen bonds in **4**. Surroundings for N8 are shown on the top, whereas surroundings for N8a are shown on the bottom. The connection site between the two motifs is transparent. Thermal ellipsoids represent the 50% probability level. Symmetry operators: i) x, $y-1$, z; ii) x, $-y+1$, $z-1/2$; iii) x, $-y+1$, $z+1/2$; iv) $-x$, y, $-z+1/2$; v) $-x$, $y+1$, $-z+1/2$; vi) $-x+1/2$, $y+1/2$, $-z+1/2$; vii) $-x+1/2$, $-y+3/2$, $-z$; viii) $-x$, $-y+1$, $-z$; ix) x, $y+1$, z.

Triaminoguanidinium 5-amino-1-nitriminotetrazolate (**8**) crystallizes in the orthorhombic space group $Pna2_1$ with a cell volume of 1009.9(2) Å^3 and four molecular moieties in the unit cell. The calculated density at 173 K is 1.639 g cm^{-3}. The asymmetric unit of **8** is presented in Figure 9.

The structure of **8** consists of ten independent hydrogen bonds, eight of which use the nitrogen atoms of the triaminoguanidinium cation as donor atoms, which connect to seven independent DATNO$_2^-$ moieties. Hence the structure presents a dense 3D hydrogen-bonded network. The hydro-
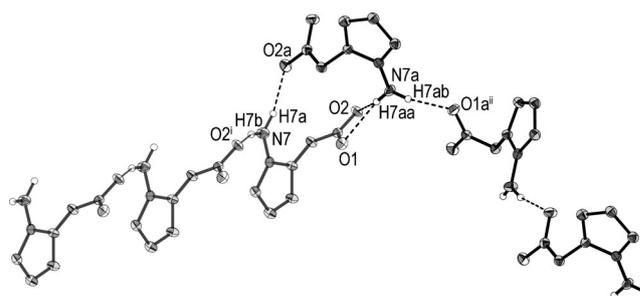
Figure 8. Rows of DATNO$_2^-$ anions formed in **4** by the two independent moieties. Ammonium cations are omitted for clarity. Thermal ellipsoids are set to 50% probability.
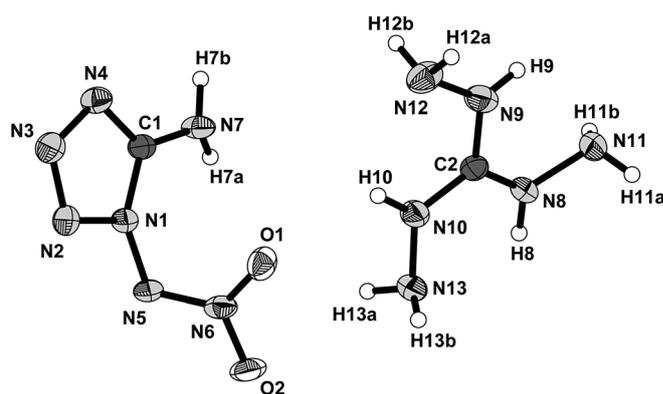
Figure 9. Asymmetric unit of **7**. Thermal ellipsoids are set to 50% probability.

gen-bonding pattern is given in Figure S4 in the Supporting Information, whereas the hydrogen bonds are compiled in Table S5 in the Supporting Information.

Spectroscopic data

Vibrational spectroscopy: IR and Raman spectra of all compounds have been recorded, and the frequencies have been assigned on the basis of the literature[24] and also on the basis of quantum mechanical calculations at the B3LYP/cc-pVDZ[25] level of theory as implemented in the Gaussian 09W program package.[26] The calculated frequencies have been fitted according to Witek et al.[27] with a scaling factor of 0.9704.

The two neutral compounds, **1** and **2**, show ν_s and ν_{as} stretching modes of the C-bound amine groups in the region of 3440–3380 cm^{-1} in both IR and Raman spectra. Additionally, the bending deformation vibrations of the amine groups are observed at 1512 (**1**) and 1515 cm^{-1} (**2**) in the IR spectra and at 1480 (**1**) and 1517 cm^{-1} (**2**) in the corresponding Raman spectra. Compound **2** showed three stretching modes (ν(C–H), ν_s(CH$_3$) and ν_{as}(CH$_3$)) of the methyl group in the region of 3350–2963 cm^{-1}. All three modes were identified in the Raman spectrum, whereas only ν_{as} was observed in the IR spectrum. Whereas the C$_{Tet}$–N5 bond stretching mode is not observed for **1**, it is clearly observed at 1690

(IR) and 1703 cm^{-1} (Raman) for **2**. The frequency values of this vibrational mode are in the region normally assigned to C=N double bonds, thereby accentuating the sp^2 character of the amine group. Vibrational modes of the nitrimine groups in **1** and **2** are observed in both the IR and Raman spectra. Compound **1** showed $\nu_{as}(NO_2)$ at 1646 cm^{-1} (IR), whereas **2** showed the stretching mode at 1665 cm^{-1} (IR). As expected, the antisymmetric stretching mode is not observed in the Raman spectra. For **1**, $\nu_s(NO_2)$ is observed at 1302 (IR) and 1307 cm^{-1} (Raman), and for **2** at 1275 (IR) and 1293 cm^{-1} (Raman). In the IR spectrum of **1**, $\nu_{as}(N1\text{-}C1\text{-}N4)$ is observed at 1448 cm^{-1}, whereas **2** shows this stretching mode in both IR and Raman spectra at 1460 and 1459 cm^{-1}, respectively. The stretching mode of the N2=N3 double bond is observed at 1400 (IR) and 1413 cm^{-1} (Raman) for **1** and at 1424 (IR) and 1427 cm^{-1} (Raman) for **2**. Whereas many out-of-plane and in-plane as well as coupled stretching and deformation modes of the tetrazole ring and its substituent are observed in the fingerprint region below 1100 cm^{-1}, one unique stretching mode can be assigned at 891 (IR) and 917 cm^{-1} (Raman) for **1** and at 898 (IR) and 902 cm^{-1} (Raman) for **2**, which represent the $\nu(N5\text{−}NO_2)$ stretching mode.

If **1** is stored at ambient temperature in humid air, two additional stretching modes are observed in the IR spectrum at 2157 and 1701 cm^{-1} together with a broadening of the $\nu_{as}(NO_2)$ band. These two bands represent a ν_{as} stretching mode of a covalently bound azide at 2157 cm^{-1}, whereas the stretching mode of a C=N double bond can be assigned at 1701 cm^{-1}. It can hence be assumed that **1** tends to decompose in humid surroundings to form nitraminoguanyl azide as a possible (intermediate) decomposition product (Scheme 5).
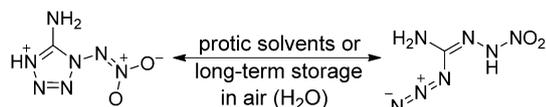
Scheme 5. Suggested decomposition (equilibrium) reaction to form nitraminoguanyl azide from 5-amino-1-nitrimino-4H-tetrazole (**1**).

The formation of the intermediate is also observed in protic solvents, and therefore no clean NMR spectra of **1** were recorded, since decomposition products were always observed too. No NMR spectrum could be recorded in aprotic solvents such as deuterated acetonitrile, the resonances being much too broad or invisible.

The salts of **1** with nitrogen-rich cations as counterions showed very broad bands of high intensity for $\nu(N\text{−}H)$, $\nu_s(NH_2)$, and $\nu_{as}(NH_2)$ in the IR spectra in the region of 3400–3040 cm^{-1}. Lines of smaller intensity are observed in the Raman spectra in the same region. Around 1500 cm^{-1} the deformation modes of the amine group are also observed. The ν_{as} stretching modes of the NO$_2$ groups are observed at 1635 (**4**), 1643 (**5**), 1645 (**6**), 1658 (**7**), and 1647 cm^{-1} (**8**) in the IR spectra and at frequency values of 1637 (**4**), 1643 (**5**),

1643 (**6**), and 1651 cm^{-1} (**7**) in the Raman spectra. Compound **8** showed too much fluorescence in this region, and the signal could not be observed. The ν_s stretching modes of the NO$_2$ groups are observed at 1296 (**4**), 1301 (**5**), 1308 (**6**), 1298 (**7**), and 1328 cm^{-1} (**8**) in the IR spectra, and at 1305 (**4**), 1302 (**5**), 1302 (**6**), 1304 (**7**), and 1324 cm^{-1} (**8**) in the Raman spectra. As observed for the neutral compounds, many coupled stretching and deformation modes of the tetrazole ring and its substituents are observed in the fingerprint region below 1100 cm^{-1}.

Multinuclear NMR spectroscopy: As seen in the vibrational spectra, a ring opening of the tetrazole backbone in **1** was observed in protic media or with longer exposure towards humidity (Scheme 5), which represents either an equilibrium or a decomposition reaction. NMR spectra of **1** show peaks assignable to the suggested decomposition product as well as **1**, but no clean NMR spectra without decomposition of **1** were recorded after numerous attempts. The amine groups of both compounds are present in the ^{1}H NMR spectrum at a chemical shift of $\delta = 5.39$ ppm as a very broad signal. The carbon atom of **1** is observed in the ^{13}C NMR spectra at a chemical shift of $\delta = 152.7$ ppm, whereas the carbon atom of the decomposition product is shifted to lower field and observed at a chemical shift of $\delta = 164.8$ ppm. The intensities of the decomposition product are much smaller than **1** close to a 1:5 ratio. Hence the azide group of the decomposition product is observed only in the ^{14}N NMR spectrum at $\delta = -143$ ppm (N$_\gamma$, br) and $\delta = -146$ ppm (N$_\beta$), whereas a very broad signal at $\delta = -300$ ppm indicates the N$_\alpha$ nitrogen atom, but not in the ^{15}N NMR spectra. The NO$_2$ group of the decomposition product is observed at a chemical shift of $\delta = -21$ ppm, whereas the NO$_2$ group of **1** is observed at $\delta = -18$ ppm. The amine group(s) are observed at a chemical shift of $\delta = -330$ ppm. The coupled and decoupled ^{15}N NMR spectra of a 1 M solution of **1** in CD$_3$OD presented no signals of the azide group due to the low concentration of the decomposition product, but revealed the signal of the NO$_2$ group in the coupled spectrum at a chemical shift of $\delta = -18.3$ ppm and the resonance of the amine group at a chemical shift of $\delta = -331.7$ ppm in the decoupled ^{15}N NMR spectrum. According to the ^{15}N NMR spectra of the educt, 1,5-diamino-tetrazole,[21b] and with calculations performed at the MPW1PW91/cc-pVDZ level of theory, the resonances of the individual nitrogen atoms of compound **1** were assigned. Resonances are observed at chemical shifts of $\delta = -18.0$, -26.1 -28.0, -161.5, -176.7, and -334.1 ppm, which represent the N6 (NO$_2$), N2, N3, N5, N1, and N7 (NH$_2$) nitrogen atoms in the coupled ^{15}N NMR spectrum. Additionally, the N4 nitrogen atom is present in the decoupled ^{15}N NMR spectrum at a chemical shift of $\delta = -56.4$ ppm. The resonance of the N5 atom is not observed in the decoupled spectrum, but the resonances of the N6 (NO$_2$), N2, N3, N1, and N7 (NH$_2$) atoms are observed at chemical shifts of $\delta = -17.5$, -26.0, -28.1, -177.7, and -331.5 ppm, respectively.

The signals of the amine groups of the DATNO$_2^-$ moieties in **4**–**8** are observed in the ^{1}H NMR spectra at chemical

shifts between $\delta = 6.10$ and 6.14 ppm. Additionally, signals are observed for the hydrogen atoms located on the cations at chemical shifts of $\delta = 7.14$ ppm for the ammonium cation (**4**); $\delta = 7.05$ ppm for the hydrazinium cation (**5**); $\delta = 6.94$ ppm for the guanidinium cation (**6**); $\delta = 8.88$ ($-NH-NH_2$), 7.24 ($-NH_2$), 6.83 ($-NH_2$), and 4.68 ppm ($-NH_2$) for the aminoguanidinium cation (**7**); and $\delta = 8.58$ ($-NH-NH_2$) and 4.48 ppm ($-NH_2$) for the triaminoguanidinium cation (**8**), respectively.

The signal of the carbon atom of the $DATNO_2^-$ anion is observed at a chemical shift of $\delta = 152.6$ ppm for all ionic compounds **4–8** in the ^{13}C NMR spectra. Signals for the carbon-containing cations are additionally observed in the ^{13}C NMR spectra at chemical shifts of $\delta = 157.9$ ppm for the guanidinium cation (**6**), $\delta = 158.8$ ppm for the aminoguanidinium cation (**7**), and $\delta = 159.0$ ppm for the triaminoguanidinium cation (**8**).

The N6 nitrogen atom ($-NO_2$) of the $DATNO_2^-$ anions is observed at a chemical shift of $\delta = -4$ ppm for all ionic compounds **4–8**. Compound **4** shows an additional signal at a chemical shift of $\delta = -359$ ppm, which represents the ammonium cation, whereas the hydrazinium cation is observed at the same chemical shift in the spectrum of **5**. The NH_2 group nitrogen atom of the $DATNO_2^-$ moiety is only observed in the ^{14}N NMR spectrum of **5** at a chemical shift of $\delta = -334$ ppm.

Additionally, ^{15}N NMR spectra were recorded for triaminoguanidinium 5-amino-1-nitriminotetrazolate as an example of the ionic compounds of **1**. All nitrogen atoms have been assigned using the combination of both coupled and decoupled ^{15}N NMR spectra. The N6 nitrogen atom (NO_2) is observed at a chemical shift of $\delta = -2.9$ ppm in both ^{15}N and $^{15}N\{^1H\}$ NMR spectra. The nitrogen atoms of the tetrazole ring N1, N2, N3, and N4 showed signals at chemical shifts of $\delta = -174.3$, -5.9, -23.6, and -96.7 ppm in the decoupled spectrum. The signal of the N1 nitrogen atom is not observed in the coupled ^{15}N NMR spectrum, whereas N2, N3, and N4 are clearly observed at chemical shifts of $\delta = -5.9$, -23.6, and -95.7 ppm. The amine group bound to the C1 atom is observed at chemical shifts of $\delta = -338.8$ ppm in both ^{15}N NMR spectra. The nitrogen atoms of the triaminoguanidinium cation showed two signals in both ^{15}N NMR spectra at chemical shifts of $\delta = -289.1$ ($-NH-$) and -329.5 ppm ($-NH_2$). The signals represent a doublet and a triplet for the $-NH-$ and $-NH_2$ nitrogen atoms, respectively, in the proton-coupled ^{15}N NMR spectrum, which shows ^1J coupling constants of $^1J(N,H) = 102.5$ Hz for the doublet and $^1J(N,H) = 69.8$ Hz for the triplet (Figure 10). Both coupling constants are in the region observed normally for $^1J(N,H)$ coupling constants.[24]

The methyl and amine group in **2** are observed in the ^1H NMR spectrum at chemical shifts of $\delta = 8.88$ (NH_2) and 3.84 ppm (CH_3). The shift towards lower field for the amine group is due to the positive charge located on the nitrogen atom, which results in a deshielding of the hydrogen atoms. Two signals are observed in the ^{13}C NMR spectrum of **2** for the tetrazole carbon at a chemical shift of $\delta = 145.6$ ppm and
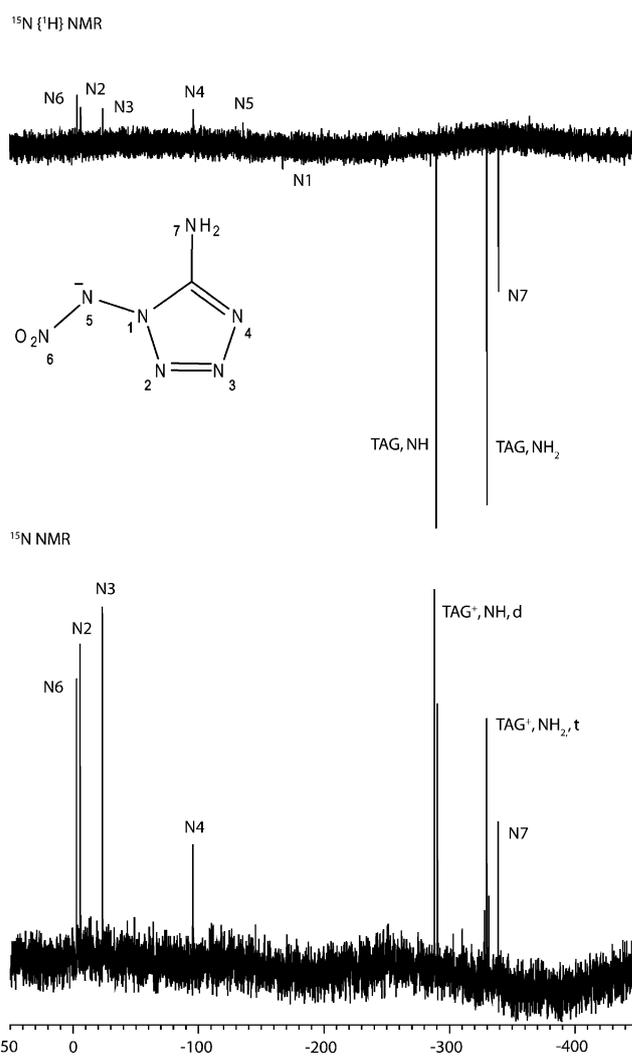

Figure 10. ^{15}N and $^{15}N\{^1H\}$ NMR spectra of triaminoguanidinium 5-amino-1-nitriminotetrazolate (**8**) recorded in [D_6]DMSO at 25 °C. The x axis represents the chemical shift (δ) [ppm].

the methyl group at $\delta = 34.4$ ppm. The tetrazole carbon atom is shifted to higher field than the neutral compound (MeDAT) at $\delta = 148.5$ ppm. Only the signal for the nitramine (NO_2) nitrogen atom is observed in the ^{14}N NMR spectrum at $\delta = -3$ ppm.

The signals of all nitrogen atoms contained in **2** have been assigned using proton-coupled and -decoupled ^{15}N NMR spectroscopy together with calculations of the nitrogen NMR spectra at the MPW1PW91/cc-pVDZ level of theory. The proton-coupled ^{15}N NMR spectrum showed, as expected, seven well-resolved resonances at higher field. N6 (NO_2) is observed at $\delta = -2.3$ ppm. The N2 and N3 nitrogen atoms are observed as a singlet and a quadruplet, respectively, at chemical shifts of $\delta = -26.1$ and -36.2 ppm. The quadruplet is observed due to the ^3J coupling of the nitrogen atom with the methyl group attached to N4 with a coupling constant of $^3J(N,H) = 1.86$ Hz. The N5 nitrogen atom is observed at a chemical shift of $\delta = -126.9$ ppm, whereas the N1 nitrogen

atom is observed at $\delta = -147.1$ ppm. N4 showed no coupling towards the attached methyl group and is found at a chemical shift of $\delta = -185.5$ ppm. The amine group showed a triplet in the proton-coupled ^{15}N NMR spectrum at -320.0 ppm that displayed a coupling constant of $^1J(N,H) = 91.29$ Hz, as expected. All seven resonances are also observed in the proton-decoupled ^{15}N NMR spectra at chemical shifts of $\delta = -2.2$ (N6), -26.0 (N2), -36.2 (N3), -126.9 (N5), -147.3 (N1), -185.5 (N4), and -320.5 ppm (N7). The spectra are compiled in Figure 11.
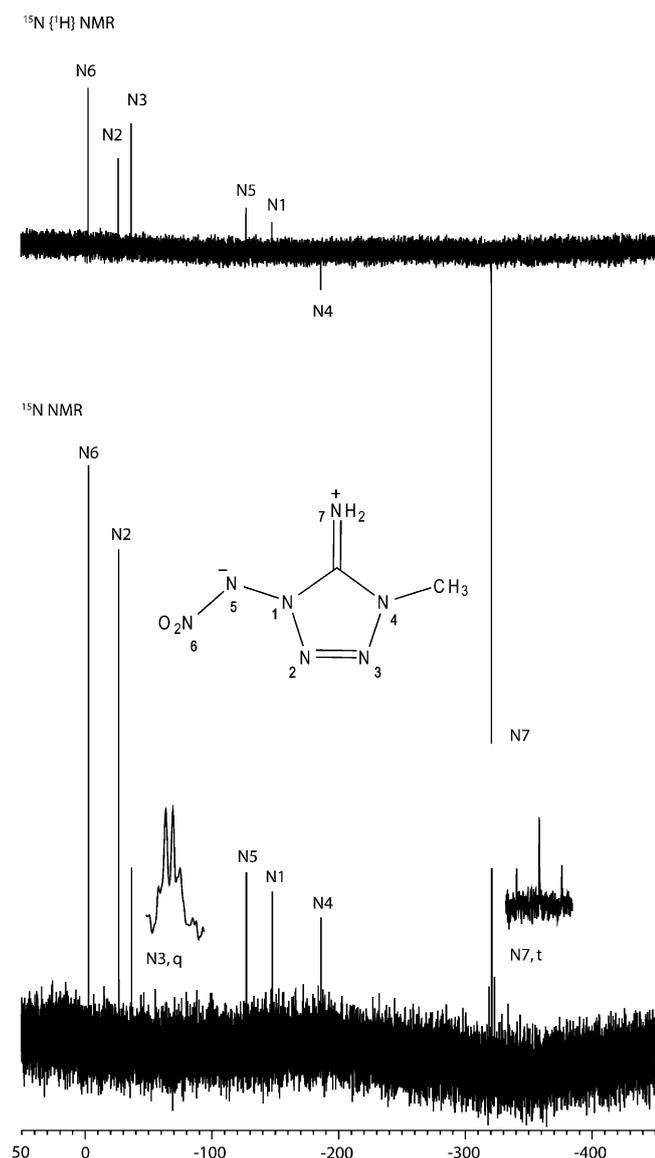
Figure 11. ^{15}N and ^{15}N{^{1}H} NMR spectra of 5-amino-4-methyl-1-nitriminotetrazole (**2**) recorded in [D$_6$]DMSO at 25 °C. The x axis represents the chemical shift (δ) [ppm].

Mass spectrometry: Mass spectra were recorded using the FAB+ and FAB− techniques for all ionic compounds, as well as **2**, in glycerin matrix. The anion of **1** (DATNO$_2^-$) was always observed at m/z 144.0 in the FAB− spectra, whereas the cations were observed at m/z 18.0 (**4**), 33.0 (**5**), 60.1 (**6**), 75.1 (**7**), and 105.13 (**8**). Compound **2** is observed in both FAB+ and FAB− spectra at m/z 160.1 [M+H]$^+$ and at m/z 158.0 [M−H]$^-$. Additionally, **1** is observed using the DCI$^+$ technique at m/z 146.03 [M+H]$^+$. During the investigation and characterization of **1** with DEI$^+$ methods, an explosion took place due to the high heating rates used for the measurements, therefore no additional information about the fragmentation pattern was gathered from these measurements.

Theoretical calculations and stabilities: All calculations for energies of formation were carried out using the Gaussian G09W version 7.0 program package.[26] Since very detailed descriptions of the calculation process have been published earlier[28] and can be found in specialized books,[3] only a short summary of computational methods will be given. The enthalpies (H) and Gibbs free energies (G) were calculated using the complete basis set method (CBS) of Petersson et al. to obtain very accurate energies. In this contribution, we used the modified CBS-4M method with M referring to the use of minimal population localization, which is a reparameterized version of the original CBS-4 computational method and also includes additional empirical calculations.[29]

The enthalpies of formation for the gas-phase species were computed according to the atomization energy method by using National Institute of Standards and Technology (NIST)[30] values as standardized values for the atoms standard heats of formation ($\Delta_f H^0$) according to Equation (1).[31]

$$\Delta_f H^{\circ}_{(g, \text{molecule}, 298)} = H_{(\text{molecule})} - \sum H^{\circ}_{(\text{atoms})} + \sum \Delta_f H^{\circ}_{(\text{atoms, NIST})} \tag{1}$$

The solid-state enthalpy of formation for neutral compounds is estimated from the computational results by using Trouton's rule,[32] for which T_m was taken to be equal to the decomposition temperatures [Eq. (2)].

$$\Delta H_m = \Delta_f H^{\circ}_{(g, 298)} - \Delta H_{\text{sub}} = \Delta_f H^{\circ}_{(g, 298)} - (188 \text{ J mol}^{-1} \text{ K}^{-1} \times T_m) \tag{2}$$

The solid-state enthalpies of formation for the ionic compounds are derived from the calculation of the corresponding lattice energies (U_L) and lattice enthalpies (H_L), calculated from the corresponding molecular volumes,[33] by the equations provided by Jenkins et al..[34]

The derived molar standard enthalpies of formation for the solid state (ΔH_m) were used to calculate the solid-state energies of formation (ΔU_m) according to Equation (3), with Δn being the change of moles of gaseous components.[3]

$$\Delta U_m = \Delta H_m - \Delta nRT \tag{3}$$

The calculated standard energies of formation were used to

perform predictions of the detonation parameters with the program package EXPLO5 (version 5.04).[35] The program is based on the chemical equilibrium, steady-state model of detonation. It uses Becker–Kistiakowsky—Wilson's equation of state (BKW EOS) for gaseous detonation products together with Cowan—Fickett's equation of state for solid carbon.[36] The calculation of the equilibrium composition of the detonation products is performed by applying modified White, Johnson, and Dantzig's free-energy minimization technique. The program was designed to enable calculations of detonation parameter at the Chapman–Jouguet point. The BKW equation as implemented in the EXPLO5 program was used with the BKW-G set of parameters (α, β, κ, θ) as stated below Equation (4), with X_i being the mole fraction of the ith gaseous detonation product, whereas k_i is the molar co-volume of the ith gaseous detonation product.[35,36]

$$pV/RT = 1 + xe^{\beta x} \qquad (4)$$

in which $x = (\kappa \Sigma X_i k_i)/[V(T+\theta)]^{\alpha}$, $\alpha = 0.5$, $\beta = 0.096$, $\kappa = 17.56$, and $\theta = 4950$. The results of the detonation runs together with the calculated energies of formation, the corresponding sensitivities, and decomposition temperatures are compiled in Table 5.

HDATNO$_2$ (**1**) shows a very low decomposition temperature of only 85 °C as a neutral compound due to the very high acidity of the hydrogen atom located at the 4-position. Upon deprotonation of **1**, the decomposition temperatures increase depending on the cation. Ammonium 5-amino-1-nitriminotetrazolate (**4**) shows the lowest decomposition temperature (only 107 °C), whereas triaminoguanidinium 5-amino-1-nitriminotetrazolate (**8**) exhibits the highest decomposition temperature of 160 °C. The decomposition tempera-

tures for compounds **5**, **6**, and **7** are 134, 148, and 142 °C, respectively. Even though 5-amino-4-methyl-1-nitriminotetrazole (**2**) is a neutral nitrimino compound, it displays a very high thermal stability with decomposition starting at 150 °C, whereas the onset value is 160 °C. Compound **2** derives its stability towards heat from its zwitterionic character and the +I effect of the methyl group, which donates electron density to the electron-deficient tetrazole ring. The differential scanning calorimetry (DSC) plots of selected compounds are shown in Figure 12.

The friction and impact sensitivities of all compounds have been determined for the anhydrous materials and show a very wide spread. Although both are neutral compounds, **1** and **2** are extremely sensitive (impact sensitivity (IS)/friction sensitivity (FS): < 0.25 J/< 5 N (**1**); < 1 J/< 5 N (**2**)), and therefore more sensitive than lead azide. The salts show no observable trend. Whereas **4** and **5** (ammonium and hydrazinium as cations) are extremely sensitive towards impact (3 J (**4**), < 1 J (**5**)) and very sensitive towards friction (52 N (**4**), 48 N (**5**)), the guanidinium and aminoguanidinium 5-amino-1-nitriminotetrazolates point in the other direction. Compounds **6** and **7** are both less sensitive towards impact (40 J (**6**), 20 J (**7**)) and also show much lower sensitivity towards friction (240 N (**6**), 192 N (**7**)). The result for the testing of the triaminoguanidinium salt (**8**) was not really as expected: it is again very sensitive towards friction at 32 N and extremely sensitive towards impact at only 2 J. Since **8** shows the highest thermal stability, we had hoped for a better value. It seems that the reductive properties of the hydrazine moieties in the triaminoguanidinium cation promote the decomposition of the nitramine moiety and therefore affect the stabilities.

From the calculation of the detonation parameter, we observe the expected picture. As a result of the high density

Table 5. Physicochemical properties of compounds **1**, **2**, and **4–8** in comparison with hexogen (RDX).

	1	**2**	**4**	**5**	**6**	**7**	**8**	RDX[a]
formula	$CH_3N_7O_2$	$C_2H_5N_7O_2$	$CH_6N_8O_2$	$CH_7N_9O_2$	$C_2H_8N_{10}O_2$	$C_2H_9N_{11}O_2$	$C_2H_{11}N_{13}O_2$	$C_3H_6N_6O_6$
M_r [g mol^{-1}]	145.1	159.1	162.1	177.1	204.2	219.2	249.2	222.1
IS [J][b]	< 0.25	< 1	3	< 1	40	20	2	7
FS [N][c]	< 5	< 5	52	48	240	192	32	120
ESD test [J]	0.025	0.211	0.20	0.10	0.26	0.20	0.065	–
N [%][d]	67.6	61.6	69.1	71.1	68.6	70.3	73.1	37.8
Ω [%][e]	−16.5	−45.2	−29.6	−31.6	−47.0	−47.5	−48.1	−21.6
m.p. (decomp) [°C][f]	85	150	107	134	148	142	160	204
ρ_{calcd} [g cm^{-3}][g]	1.835	1.643	1.757	1.678	1.619	1.649	1.639	1.80
$\Delta_f H_m^{\circ}$ [kJ mol^{-1}][h]	496	453	356	516	343	451	676	70
$\Delta_f U^{\ominus}$ [kJ kg^{-1}][i]	3419	2847	2195	2911	1678	2059	2711	417
EXPLO5 values (v5.04)								
$-\Delta_E U^{\ominus}$ [kJ kg^{-1}][j]	6498	5913	5326	5856	4299	4564	5023	6125
T_E [K][k]	4642	3969	3613	3806	3072	3116	3297	4236
$p_{C–J}$ [kbar][l]	403	292	344	334	255	276	295	349
v_{det} [m s^{-1}][m]	9460	8561	9111	9102	8168	8465	8731	8748
gas volume [L kg^{-1}][n]	805	798	875	886	843	854	871	739

[a] Values based on Ref. [37] and the EXPLO5 database; n.d.: not determined. [b] IS = impact sensitivity; BAM drop hammer, grain size (75–150 μm). [c] FS = friction sensitivity; BAM friction tester, grain size (75–150 μm). [d] Nitrogen content. [e] Oxygen balance.[40] [f] Temperature of decomposition by DSC ($\beta = 5$ °C, onset values). [g] Density calculated from X-ray measurements. [h] Molar enthalpy of formation. [i] Energy of formation. [j] Energy of explosion. [k] Explosion temperature. [l] Detonation pressure. [m] Detonation velocity. [n] Assuming only gaseous products.
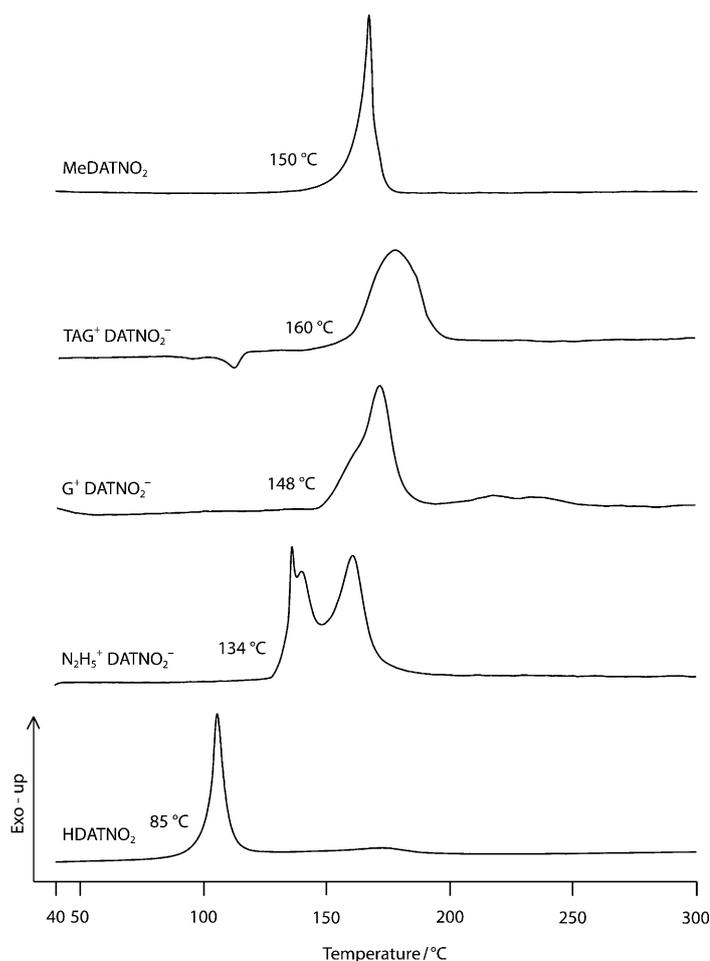
Figure 12. DSC plots of HDATNO₂ (**1**), N₂H₅⁺ DATNO₂⁻ (**5**), G⁺ DATNO₂⁻ (**6**), TAG⁺ DATNO₂⁻ (**8**), and MeDATNO₂ (**2**) recorded at a heating rate of 5 °C min⁻¹.

and high heat of formation, compound **1** is extremely powerful and exceeds the performance characteristics of RDX by far ($v_{det} = 9460$ m s⁻¹ (**1**), 8748 m s⁻¹ (RDX)). The same is observed for **4** and **5**, which display detonation velocities of 9110 and 9102 m s⁻¹ along with an enormous amount of gas release (875 L kg⁻¹ (**4**); 886 L kg⁻¹ (**5**)) and detonation pressures of 344 and 334 kbar, respectively. These values in addition to the ones for **8** ($v_{det} = 8731$ m s⁻¹; $p_{C-J} = 295$ kbar; 871 L kg⁻¹) are in the range of RDX values or even exceed them. The drawback is that all these compounds are, as described above, very sensitive towards both impact and friction, and despite a reasonably good thermal stability for **8** are not very safe in use and handling. Compounds **6** and **7** display mean sensitivity values and are therefore easy to handle, but show only reasonable performance characteristics, well below the benchmark values of RDX.

Conclusion

Two novel N-bound primary nitramines have been synthesized in good yields by the reaction of 1,5-diaminotetrazole

and 1-amino-5-imino-4-methyltetrazole with the mild nitrating reagent nitronium tetrafluoroborate. Both compounds **1** and **2** exhibit very high sensitivities to friction, impact, and electrostatic discharge, yet they have been fully characterized by means of vibrational and multinuclear NMR spectroscopy and also by mass spectrometry. The decomposition reaction of **1** in protic solvents has also been investigated by means of vibrational and ¹⁵N/¹H/¹³C NMR spectroscopy. Compounds **1** (85 °C) and **2** (150 °C) differ very much in decomposition temperature (65 °C), a result of the introduction of the methyl group on the 4-position. Both neutral compounds have also been investigated by means of single-crystal X-ray diffraction measurements.

The energetic ionic compounds composed of **1** and the corresponding nitrogen-rich cations have been synthesized by metathesis reactions from different solvents. All ionic compounds (**4–8**) have been crystallized as anhydrous compounds from various solvents, and single-crystal X-ray diffraction measurements of all compounds have been performed. The characterization of **4–8** by using vibrational and multinuclear NMR spectroscopy as well as mass spectrometry has been undertaken. Additionally, quantum mechanical calculations have been performed to obtain reasonable heats of formations for all compounds, since the highly energetic character of the salts prohibits the use of combustion experiments by bomb calorimetry. The densities derived from single-crystal X-ray measurements have been used together with the calculated heats of formation to derive detonation parameters for all compounds (**1**, **2**, **4–8**) with the EXPLO5 version 5.04 code. Whereas **4** and **5** show very good performance data for the detonation velocity (9111 (**4**) and 9102 m s⁻¹ (**5**)) and detonation pressure (344 (**4**), 334 kbar (**5**)), they are on the other hand much too sensitive to friction and impact and decompose at low temperatures of only 107 (**4**) and 134 °C (**5**). Compounds **6** and **7** exhibit mean sensitivities to friction and impact but show much lower values for detonation velocity and detonation pressure. The best-performing compound in terms of thermal stability is triaminoguanidinium 5-amino-1-nitriminotetrazolate (**8**). It exhibits a decomposition temperature of 160 °C and shows promising values derived from performance calculations ($v_{det} = 8731$ m s⁻¹; $P_{C-J} = 295$ kbar; $v_0 = 871$ L kg⁻¹) but unfortunately also exhibits very high sensitivities to friction and impact with 32 N and 2 J, respectively. Some compounds (**1**, **4**, **5**, and **8**) show performance characteristics well above the values of RDX, but are too sensitive for use and handling and do not exhibit very high thermal stabilities.

Experimental Section

standards, and coupling constants are given in Hertz (Hz). Infrared (IR) spectra were recorded using a Perkin–Elmer Spectrum BX FTIR instrument equipped with an ATR unit at 25 °C. Transmittance values are qualitatively described as "very strong" (vs), "strong" (s), "medium" (m), "weak" (w), and "very weak" (vw). Raman spectra were recorded using a Bruker RAM II spectrometer equipped with an Nd:YAG laser operating at 1064 nm and a reflection angle of 180°. The intensities are reported as percentages of the most intense peak and are given in parentheses. The laser energy was set to 200 mW for all compounds. Elemental analyses (CHNO) were performed using a Netzsch Simultaneous Thermal Analyzer STA 429. Melting and decomposition points were determined by differential scanning calorimetry (Linseis PT 10 DSC, calibrated with standard pure indium and zinc). Measurements were performed at a heating rate of 5 °C min^{-1} in closed aluminum sample pans with a 1 µm hole in the top for gas release to avoid an unsafe increase in pressure under a nitrogen flow of 20 mL min^{-1} with an empty identical aluminum sample pan as a reference. The mass spectra were recorded with desorption electron ionization (DEI) and desorption chemical ionization (DCI) methods using a JEOL MStation JMS 700 mass spectrometer.

For initial safety testing, the impact and friction sensitivities as well as the electrostatic sensitivities were determined. The impact sensitivity tests were carried out according to STANAG 4489,[38] which were modified according to Wehrwissenschaftliches Institut der Bundeswehr (WIWEB) instruction 4-5.1.02[39] using a BAM[40] drop hammer. The friction sensitivity tests were carried out according to STANAG 4487[41] and modified according to WIWEB instruction 4-5.1.03[42] using a BAM friction tester. The electrostatic sensitivity tests were accomplished according to STANAG 4490[43] using an electric spark testing device ESD 2010EN (OZM Research) operating with the Winspark 1.15 software package.[44]

Crystallographic measurements: The single-crystal X-ray diffraction data of **1**, **2**, and **4–8** were collected using an Oxford Xcalibur3 diffractometer equipped with a Spellman generator (voltage 50 kV, current 40 mA) and a KappaCCD detector. The data collection was undertaken using the Crysalis CCD software[45] while the data reduction was performed with the Crysalis RED software.[46] The structures were solved with SIR-92[47] or SHELXS-97[48] and refined with SHELXL-97[49] implemented in the program package WinGX[50] and finally checked using PLATON.[51]

CCDC-824129 (**1**), 824135 (**2**), 824133 (**4**), 824134 (**5**), 824131 (**6**), 824130 (**7**), and 824132 (**8**) contain the supplementary crystallographic data for this paper. These data can be obtained free of charge from The Cambridge Crystallographic Data Centre via www.ccdc.cam.ac.uk/data_request/cif.

5-Amino-1-nitriminotetrazole (HDATNO₂, 1): 1,5-Diaminotetrazole (2 g, 20 mmol) was dissolved in dry acetonitrile (50 mL). The solution was held at 0 °C (ice-bath cooling) and nitronium tetrafluoroborate (2.65 g, 20 mmol) was added under stirring to the solution, which turned slightly yellow. The reaction mixture was allowed to stir overnight at room temperature. Acetonitrile was then evaporated under vacuum to result in a yellowish solid. The solid was redissolved in a small amount of ethanol (5 mL), and a solution of potassium hydroxide (1.12 g, 20 mmol) in ethanol (20 mL) was added to result in the precipitation of potassium tetrafluoroborate, which was separated from the solution by filtration. The ethanolic solution was then reduced to dryness, thereby leaving a crude yellow product of HDATNO₂ (1.7 g, 59 %). The crude product was recrystallized from ethanol and ether to yield pure HDATNO₂ (1.6 g, 55 %). M.p. (decomp) 85 °C (DSC, onset, 5 °C min^{-1}); sensitivities (anhydrous) (grain size: 100–500 µm): IS < 0.25 J; FS: < 1 N; ESD: 25 mJ; ^{1}H NMR (CD₃OD, 25 °C): δ = 5.39 ppm (s, 2H; −NH₂); ^{13}C{^{1}H} NMR (CD₃OD, 25 °C): δ = 152.7 ppm; ^{14}N NMR (CD₃OD, 25 °C): δ = −18 (−N−NO₂, N6), −21 (−N−NO₂, decomp product), −143 (N$_\gamma$, decomp product), −146 (N$_\beta$, decomp product), −176 (N1), −300 (br; N$_\alpha$, decomp product), −330 ppm (NH₂, N7); ^{15}N NMR (CD₃OD, 25 °C): δ = −18.0 (N6), −18.3 (N−NO₂, decomp product), −26.1 (N2), −28.0 (N3), −161.5 (N5), −176.7 (N1), −331 ppm (NH₂, N7); ^{15}N{^{1}H} NMR (CD₃OD, 25 °C): δ = −17.5 (−N−NO₂, N6), −26.0 (N2), −28.1 (N3), −56.4 (N4), −177.7 (N1), −331.5 (NH₂, N7), −334.1 ppm (NH₂, decomp product); IR (ATR, 25 °C): ṽ = 3424 (m), 3335 (m), 3262 (m), 1705 (m), 1645 (m), 1495 (w), 1445 (mw), 1384 (vs), 1302 (m), 1259 (w), 1102 (w), 1050 (w), 1039 (w),

976 (vw), 838 (vw), 727 (vw), 710 cm^{-1} (vw); IR (Raman) (Nd:YAG, 1064 nm): ṽ = 3304 (2), 3250 (8), 3150 (1), 1710 (3), 1697 (3), 1583 (7), 1481 (38), 1413 (5), 1373 (15), 1307 (55), 1267 (15), 1130 (21), 1084 (8), 971 (68), 917 (9), 771 (100), 716 (12), 664 (1), 829 (8), 452 (20), 415 (13), 325 (13), 275 cm^{-1} (5); DCI+: m/z: 146.03 [M+H]$^+$.

Silver 5-amino-1-nitriminotetrazolate (Ag$^+$ DATNO₂$^-$, 3): 5-Amino-1-nitriminotetrazole (0.725 g, 5 mmol) was dissolved in water (50 mL), and a solution of silver nitrate (0.934 g, 5.5 mmol) in water (25 mL) was added slowly, thus forming a gray precipitate immediately. The suspension was stirred for an additional hour under the exclusion of light. The precipitate was removed by filtration, washed with water (500 mL), and dried at 50 °C overnight to yield Ag$^+$ DATNO₂$^-$ (1.22 g, 97 %). M.p. (decomp) 158 °C (DSC, onset, 5 °C min^{-1}); sensitivities (grain size: 100–500 µm): IS: < 1 J; FS: < 5 N; IR (ATR, 25 °C): ṽ = 3431 (m), 3332 (m), 3203 (w), 3140 (w), 1655 (vs), 1647 (vs), 1546 (w), 1462 (m), 1436 (m), 1351 (w), 1300 (s), 1255 (s), 1139 (w), 1061 (w), 903 (w), 816 (w), 768 (w), 727 cm^{-1} (w); IR (Raman) (Nd:YAG, 1064 nm): ṽ = 3329 (9), 3216(9), 1645 (35), 1575 (12), 1547 (21), 1491 (20), 1457 (30), 1354 (35), 1334 (31), 1293 (58), 1267 (22), 1243 (22), 1137 (43), 1101 (38), 1041 (48), 1012 (42), 993 (94), 902 (28), 778 (100), 728 (9), 713 (9), 547 (14), 463 (25), 422 (20), 327 (16), 296 cm^{-1} (16).

General procedure for ionic compounds 4–7: Compound **3** (1.02 g, 4 mmol) was suspended in water (5 mL), and a solution of the corresponding halides (3.2 mmol) in water (5 mL) was added slowly. The suspensions were left stirring for 2 h under the exclusion of light, and the resulting silver chloride (**4**, **5**) or bromide (**6**, **7**) was removed by vacuum filtration. Ethanol (90 mL) was added to each filtrate, and the volumes of the resulting solutions were reduced in vacuum to $^1/_4$ of their original volume and left standing for crystallization. The deposited crystals of **4–7** were removed by filtration and washed thoroughly with diethyl ether.

Ammonium 5-amino-1-nitriminotetrazolate (NH₄$^+$ DATNO₂$^-$, 4): Colorless crystals. Yield: 0.432 g (83.5 %). M.p. (decomp) 107 °C (DSC, onset, 5 °C min^{-1}); sensitivities (monohydrate) (grain size: 100–500 µm): IS: 3 J; FS: 52 N; ESD: 200 mJ; ^{1}H NMR ([D₆]DMSO, 25 °C): δ = 7.13 (s, 4H; NH₄$^+$), 6.14 ppm (s, 2H; −NH₂); ^{13}C{^{1}H} NMR ([D₆]DMSO, 25 °C): δ = 152.6 ppm; ^{14}N NMR ([D₆]DMSO, 25 °C): δ = −4 (−N−NO₂), −138, −359 ppm (NH₄$^+$); IR (ATR, 25 °C): ṽ = 3359 (m), 3235 (s), 3182 (s), 3039 (s), 2857 (m), 1635 (m), 1578 (w), 1418 (m), 1378 (m), 1296 (m), 1261 (m), 1121 (w), 1070 (w), 1000 (w), 901 (w), 871 (w), 825 (w), 736 cm^{-1} (w); IR (Raman) (Nd:YAG, 1064 nm): ṽ = 3241 (7), 3186 (9), 3059 (4), 1678 (3), 1637 (18), 1577 (12), 1470 (28), 1451 (25), 1322 (18), 1305 (41), 1264 (39), 1132 (25), 1082 (9), 1044 (17), 1023 (100), 1011 (83), 989 (30), 903 (10), 875 (13), 769 (64), 757 (39), 721 (21), 680 (3), 532 (17), 466 (7), 447 (9), 419 (8), 392 (28), 339 (18), 320 cm^{-1} (13); FAB+: m/z: 18.0 [NH₄]$^+$; FAB−: m/z: 144.0 [DATNO₂]$^-$; elemental analysis calcd (%) for CH₆N₈O₂·1 H₂O: C 6.67, H 4.48, N 62.21; found: C 6.67, H 4.33, N 60.23.

Hydrazinium 5-amino-1-nitriminotetrazolate (N₂H₅$^+$ DATNO₂$^-$, 5): Light yellow crystals. Yield: 0.403 g (71 %). M.p. (decomp) 134 °C (DSC, 5 °C min^{-1}), 151 °C (DSC, onset, 5 °C min^{-1}); sensitivities (anhydrous) (grain size: 100–500 µm): IS: < 1 J; FS: 48 N; ESD: 100 mJ; ^{1}H NMR ([D₆]DMSO, 25 °C): δ = 7.03 (s, 5H; N₂H₅$^+$), 6.12 ppm (s, 2H; −NH₂); ^{13}C{^{1}H} NMR ([D₆]DMSO, 25 °C): δ = 152.6 ppm; ^{14}N NMR ([D₆]DMSO, 25 °C): δ = −4 (N−NO₂), −138, −334, −359 ppm (N₂H₅$^+$); IR (ATR, 25 °C): ṽ = 3430 (s), 3317 (s), 3284 (vs), 3260 (s), 3196 (s), 3160 (s), 1643 (s), 1574 (m), 1548 (m), 1467 (m), 1386 (s), 1301 (s), 1248 (s), 1143 (w), 1110 (m), 1094 (m), 1053 (m), 1012 (vw), 982 (m), 893 (m), 826 (w), 779 (w), 758 (w), 730 (w), 676 cm^{-1} (w); IR (Raman) (Nd:YAG, 1064 nm): ṽ = 3287 (4), 3265 (4), 3211 (6), 3179 (4), 1643 (5), 1629 (5), 1572 (8), 1455 (15), 1412 (3), 1357 (3), 1324 (21), 1302 (20), 1263 (7), 1155 (6), 1127 (13), 1056 (6), 1012 (100), 986 (42), 896 (10), 761 (50), 725 (8), 537 (7), 455 (9), 403 (6), 327 (10), 296 cm^{-1} (6); FAB+: m/z: 33.0 [N₂H₅]$^+$; FAB−: m/z: 144.0 [DATNO₂]$^-$; elemental analysis calcd (%) for CH₇N₉O₂: C 6.78, H 3.98, N 71.17; found: C 6.51, H 3.71, N 70.47.

Guanidinium 5-amino-1-nitriminotetrazolate (G$^+$ DATNO₂$^-$, 6): Colorless crystals. Yield: 0.485 g (74 %). M.p. (decomp) 148 °C (DSC, 5 °C min^{-1}), 159 °C (DSC, onset, 5 °C min^{-1}); sensitivities (anhydrous) (grain size: 500–1000 µm): IS: 40 J; FS: 240 N; ESD: 260 mJ; ^{1}H NMR

([D$_6$]DMSO, 25°C): $\delta = 6.94$ (s, 6H; C(NH_2)$_3^+$), 6.10 ppm (s, 2H; −NH_2); ^{13}C{^{1}H} NMR ([D$_6$]DMSO, 25°C): $\delta = 157.9$ (C(NH$_2$)$_3^+$), 152.6 ppm (DATNO$_2^-$); ^{14}N NMR ([D$_6$]DMSO, 25°C): $\delta = -4$ (N−NO$_2$), −137 ppm; IR (ATR, 25°C): $\tilde{\nu} = 3416$ (s), 3314 (s), 3254 (s), 3183 (s), 1645 (s), 1579 (m), 1512 (w), 1466 (w), 1453 (w), 1383 (m), 1308 (m), 1264 (m), 1113 (w), 1052 (w), 1013 (vw), 980 (vw), 900 (w), 774 (w), 620 cm^{-1} (vw); IR (Raman) (Nd:YAG, 1064 nm): $\tilde{\nu} = 3338$ (4), 3254 (5), 3198 (5), 2152 (2), 1643 (7), 1571 (5), 1466 (10), 1451 (16), 1326 (11), 1301 (14), 1265 (10), 1139 (5), 1115 (11), 1055 (30), 1014 (100), 902 (7), 768 (28), 724 (5), 538 (15), 525 (13), 459 (5), 417 (5), 332 cm^{-1} (4); FAB+: m/z: 60.1 [C-(NH$_2$)$_3$]$^+$; FAB−: m/z: 144.0 [DATNO$_2$]$^-$; elemental analysis calcd (%) for C$_2$H$_8$N$_{10}$O$_2$·H$_2$O: C 10.80, H 4.68, N 62.95; found: C 11.58, H 4.71, N 62.82.

Aminoguanidinium 5-amino-1-nitriminotetrazolate (AG$^+$ DATNO$_2^-$, 7): Light yellow crystals. Yield: 0.532 g (76%). M.p. (decomp) 142°C (DSC, onset, 5°C min^{-1}); sensitivities (anhydrous) (grain size: 100–500 μm): IS: 20 J; FS: 192 N; ESD: 200 mJ; ^{1}H NMR ([D$_6$]DMSO, 25°C): $\delta = 8.58$ (s, 1H; −NH−NH$_2$), 7.24 (s, 2H; −NH_2), 6.83 (s, 2H; −NH_2), 6.12 (s, 2H; −NH_2, DATNO$_2^-$), 4.68 ppm (s, 2H; −NH−NH_2); ^{13}C{^{1}H} NMR ([D$_6$]DMSO, 25°C): $\delta = 158.8$ (CH$_7$N$_4^+$), 152.6 ppm (DATNO$_2^-$); ^{14}N NMR ([D$_6$]DMSO, 25°C): $\delta = -4$ (N−NO$_2$), −138 ppm; IR (ATR, 25°C): $\tilde{\nu} = 2448$ (m), 3331 (s), 3254 (s), 3192 (s), 1658 (s), 1575 (m), 1517 (w), 1464 (m), 1405 (m), 1299 (m), 1264 (m), 1204 (w), 1069 (w), 981 (w), 891 (vw), 822 (vw), 772 (vw), 734 cm^{-1} (vw); IR (Raman) (Nd:YAG, 1064 nm): $\tilde{\nu} = 3350$ (8), 3335 (10), 3256 (10), 3227 (11), 1675 (9), 1651 (5), 1633 (5), 1589 (6), 1535 (4), 1463 (16), 1400 (2), 1304 (32), 1273 (21), 1206 (5), 1119 (12), 1074 (8), 1050 (12), 1016 (100), 992 (25), 966 (35), 893 (8), 757 (28), 722 (7), 620 (9), 534 (5), 507 (13), 466 (13), 400 (7), 341 (7), 306 cm^{-1} (4); FAB+: m/z: 75.1 [CH$_7$N$_4$]$^+$; FAB−: m/z: 144.0 [DATNO$_2$]$^-$; elemental analysis calcd (%) for C$_2$H$_9$N$_{11}$O$_2$·^{1}/$_2$H$_2$O: C 10.53, H 4.42, N 67.52; found: C 11.01, H 4.24, N 66.60.

Triaminoguanidinium 5-amino-1-nitriminotetrazolate (TAG$^+$ DATNO$_2^-$, 8): Compound 3 (1.02 g, 4 mmol) was suspended in dry MeCN (50 mL). Triaminoguanidinium chloride (0.374 g, 2.6 mmol) was added in one portion afterwards, and the reaction mixture was stirred for 4 d under the exclusion of light. The suspension was then filtered, and the residue was washed with MeCN (10 mL). The solvent was completely evaporated to leave analytically pure TAG$^+$ DATNO$_2^-$ (0.58 g, 89.5%). Crystals suitable for X-ray diffraction measurements were obtained as colorless rods after recrystallization from dry MeCN. M.p. 107°C (DSC, onset, 5°C min^{-1}); m.p. (decomp) 160°C (DSC, onset, 5°C min^{-1}); sensitivities (anhydrous) (grain size: 100–500 μm): IS: 2 J; FS: 32 N; ESD: 65 mJ; ^{1}H NMR ([D$_6$]DMSO, 25°C): $\delta = 8.58$ (s, 3H; −NH−NH$_2$), 6.07 (s, 2H; −NH$_2$, DATNO$_2^-$), 4.48 ppm (s, 6H; −NH−NH_2); ^{13}C{^{1}H} NMR ([D$_6$]DMSO, 25°C): $\delta = 159.0$ (CH$_9$N$_6^+$), 152.6 ppm (DATNO$_2^-$); ^{14}N NMR ([D$_6$]DMSO, 25°C): $\delta = -4$ ppm (−N−NO$_2$); ^{15}N{^{1}H} NMR ([D$_6$]DMSO, 25°C): $\delta = -2.9$ (−N−NO$_2$, N6), −5.9 (N2), −23.5 (N3), −96.7 (N4), −166.7 (N5), −174.3 (N1), −289.2 (CH$_9$N$_6^+$), −329.6 (CH$_9$N$_6^+$), −338.8 ppm (−NH$_2$, N7); ^{15}N NMR ([D$_6$]DMSO, 25°C): $\delta = -2.9$ (−N−NO$_2$, N6), −5.9 (N2), −23.6 (N3), −95.7 (N4), −289.1 (d, ^{1}J-(N,H) = 102.5 Hz; CH$_9$N$_6^+$), −329.5 (t, ^{1}J(N,H) = 69.8 Hz; CH$_9$N$_6^+$), −338.8 ppm (−NH$_2$, DATNO$_2^-$); IR (ATR, 25°C): $\tilde{\nu} = 3360$ (s), 3318 (vs), 3209 (vs), 1685 (s), 1647 (s), 1614 (m), 1581 (m), 1466 (w), 1401 (s), 1328 (vs), 1275 (m), 1127 (m), 1061 (w), 1022 (w), 990 (w), 951 (m), 877 (w), 766 (w), 737 (w), 672 (vw), 638 (w), 603 (m), 455 cm^{-1} (vw); IR (Raman) (Nd:YAG, 1064 nm): $\tilde{\nu} = 3256$ (74), 3233 (77), 3124 (74), 1517 (94), 1459 (98), 1325 (90), 1267 (89), 1298 (98), 1133 (82), 1086 (80), 1013 (100), 991 (90), 893 (80), 764 (79), 418 cm^{-1} (61); FAB+: m/z: 105.13 [CH$_9$N$_6$]$^+$; FAB−: m/z: 144.01 [DATNO$_2$]$^-$; elemental analysis calcd (%) for C$_2$H$_{11}$N$_{13}$O$_2$: C 9.64, H 4.45, N 73.07; found: C 10.03, H 4.64, N 73.00.

5-Amino-4-methyl-1-nitiminotetrazole (MeDATNO$_2$, 2): 1-Amino-5-imino-4-methyltetrazole (0.342 g, 3 mmol) was dissolved in MeCN (15 mL), and the solution was cooled down to 0°C. NO$_2$BF$_4$ (0.397 g, 3 mmol) was added to the solution in one portion, resulting in a slightly yellow solution. The reaction mixture was stirred at 0°C for additional 30 min, removed from the ice bath afterwards, and left stirring at room temperature for 1 h. The solution was left standing overnight; MeCN evaporated slowly. Upon complete evaporation of the solvent, MeDAT-NO$_2$ was deposited as colorless crystals. The crystals were washed with a small amount of water and ether afterwards to yield pure (by elemental analysis) MeDATNO$_2$ (0.255 g, 53%). M.p. (decomp) 150°C (DSC, 5°C min^{-1}), 163°C (DSC, onset, 5°C min^{-1}); sensitivities (anhydrous) (grain size: 100–500 μm): IS: <1 J; FS: <5 N; ESD: 211 mJ; ^{1}H NMR ([D$_6$]DMSO, 25°C): $\delta = 8.88$ (s, 2H; =NH_2^+), 3.84 ppm (s, 3H; −CH_3); ^{13}C{^{1}H} NMR ([D$_6$]DMSO, 25°C): $\delta = 145.6$, 34.4 ppm (−CH$_3$); ^{14}N NMR ([D$_6$]DMSO, 25°C): $\delta = -3$ ppm (−N−NO$_2$); ^{15}N NMR ([D$_6$]DMSO, 25°C): $\delta = -2.3$ (−N−NO$_2$, N6), −26.1 (N2), −36.2 (q, ^{3}J(N,H) = 1.86 Hz; N3), −126.9 (N5), −147.3 (N1), −185.5 (N4), −320.4 ppm (t, ^{1}J(N,H) = 91.29 Hz; N7); ^{15}N{^{1}H} NMR ([D$_6$]DMSO, 25°C): $\delta = -2.2$ (−N−NO$_2$, N6), −26.0 (N2), −36.2 (N3), −126.9 (N5), −147.3 (N1), −185.8 (N4), −320.5 ppm (=NH$_2$, N7); IR (ATR, 25°C): $\tilde{\nu} = 3241$ (m), 3198 (w), 3068 (m), 1690 (vs), 1615 (w), 1560 (vw), 1515 (w), 1424 (m), 1392 (m), 1344 (w), 1275 (vs), 1232 (s), 1113 (w), 1036 (m), 1015 (m), 982 (m), 898 (m), 791 (w), 781 (m), 737 (w), 711 (w), 682 cm^{-1} (w); IR (Raman) (Nd:YAG, 1064 nm): $\tilde{\nu} = 3246$ (3), 3047 (9), 3020 (7), 2964 (60), 2891 (2), 2831 (7), 1703 (9), 1621 (3), 1565 (4), 1518 (18), 1459 (16), 1427 (4), 1394 (28), 1345 (57), 1294 (3), 1237 (5), 1114 (19), 1039 (11), 1017 (34), 983 (66), 903 (11), 792 (100), 742 (18), 681 (4), 543 (5), 455 (16), 405 (17), 342 (8), 300 cm^{-1} (25); FAB+: m/z: 160.1 [M+H]$^+$; FAB−: m/z: 158.0 [M−H]$^-$; elemental analysis calcd (%) for C$_2$H$_5$N$_7$O$_2$: C 15.10, H 3.17, N 61.62; found: C 15.70, H 2.91, N 60.40.

[1] J. Wilbrand, *Liebigs Ann. Chem.* **1863**, *128*, 178–179.

[2] a) R. Meyer, J. Köhler, A. Homburg, *Explosives*, Sixth ed., Wiley-VCH Verlag GmbH & Co. KGaA, Weinheim, **2007**; b) J. A. Zukas, W. P. Walters, *Explosive effects and applications*, Springer, Heidelberg, New York, **1998**.

[3] T. M. Klapötke, *Chemie der hochenergetischen Materialien*, 1 ed., Walter de Gruyter, Berlin, New York, **2009**.

[4] a) H. Feuer, A. T. Nielsen, *Nitro compounds*, Wiley-VCH, Weinheim, **1990**; b) A. T. Nielsen, *Nitrocarbons*, Wiley-VCH, Weinheim, **1995**.

[5] a) N. V. Latypov, U. Wellmar, P. Goede, A. J. Bellamy, *Org. Process Res. Dev.* **2000**, *4*, 156–158; b) A. T. Nielsen, US 5,693,794, **1997**.

[6] M.-X. Zhang, P. E. Eaton, R. Gilardi, *Angew. Chem.* **2000**, *112*, 422–426; *Angew. Chem. Int. Ed.* **2000**, *39*, 401–404.

[7] R. L. Simpson, P. A. Urtiew, D. L. Ornellas, G. L. Moody, K. J. Scribner, D. M. Hoffman, *Propellants Explos. Pyrotech.* **1997**, *22*, 249–255.

[8] V. A. Ostrovskii, M. S. Pevzner, T. P. Kofman, I. V. Tselinskii, *Targets Heterocyclic System* **1999**, Volume 3, pp. 467–526.

[9] M. B. Talawar, R. Sivabalan, T. Mukundan, H. Muthurajan, A. K. Sikder, B. R. Gandhe, A. S. Rao, *J. Hazard. Mater.* **2009**, *161*, 589–607.

[10] W. D. Won, L. H. DiSalvo, J. Ng, *Appl. Environ. Microbiol.* **1976**, *31*, 576–580.

[11] T. E. O'Connor, G. Flemming, J. Reilly, *J. Soc. Chem. Ind. (London)* **1949**, *68*, 309–310.

[12] a) E. Lieber, E. Sherman, S. H. Sherman, *J. Am. Chem. Soc.* **1951**, *73*, 2329–2331; b) E. Lieber, E. Sherman, R. A. Henry, J. Cohen, *J. Am. Chem. Soc.* **1951**, *73*, 2327–2329; c) R. M. Herbst, J. Garrison, *J. Org. Chem.* **1953**, *18*, 941–945.

[13] J. A. Garrison, R. M. Herbst, *J. Org. Chem.* **1957**, *22*, 278–283.

[14] a) R. Damavarapu, T. M. Klapötke, J. Stierstorfer, K. R. Tarantik, *Propellants Explos. Pyrotech.* **2010**, *35*, 395–406; b) T. M. Klapötke, J. Stierstorfer, A. U. Wallek, *Chem. Mater.* **2008**, *20*, 4519–4530; c) T. M. Klapötke, in *High Energy Density Materials* (Ed.: T. M. Klapötke), Springer, Heidelberg, **2007**, pp. 84–122; d) J. Stierstorfer, T. M. Klapötke, *Helv. Chim. Acta* **2007**, *12*, 2132; e) J. Stierstorfer, K. R. Tarantik, T. M. Klapötke, *Chem. Eur. J.* **2009**, *15*, 5775–5792.

[15] T. P. Kofman, G. Y. Kartseva, M. B. Shcherbinin, *Russ. J. Org. Chem.* **2002**, *38*, 1343–1350.

[16] a) A. I. Glushkov, O. P. Shitov, V. A. Tartakovsky, *Russ. Chem. Bull.* **2003**, *52*, 467–470; b) Y. Huang, H. Gao, B. Twamley, J. M. Shreeve, *Eur. J. Inorg. Chem.* **2008**, 2560–2568; c) A. R. Katritzky, G. L. Sommen, A. V. Grovoma, R. M. Witek, P. J. Steel, R. Damavarapu, *Chem. Heterocyc. Comp.* **2005**, *41*, 111–118; d) O. Shitov, V. Korolev, V. Tartakovsky, *Russ. Chem. Bull.* **2009**, *58*, 2347–2355; e) O. P. Shitov, V. L. Korolev, V. S. Bogdanov, V. A. Tartakovsky, *Russ. Chem. Bull.* **2003**, *52*, 695–699; f) C.-R. Zhang, Y.-L. Wang, *Synth. Commun.* **2003**, *33*, 4205–4208.

[17] a) R. Damavarapu, in 37th ICT - Energetic Materials, **2006**, pp. 17/11–17/15; b) R. Duddu, P. R. Dave, R. Damavarapu, N. Gelber, D. Parrish, *Tetrahedron Lett.* **2010**, *51*, 399–401.

[18] M. A. Ilyushin, A. N. Terpigorev, I. V. Tselinskii, *Russ. J. Gen. Chem.* **1999**, *69*, 1654–1657.

[19] a) Z. X. Chen, J. M. Xiao, H. M. Xiao, Y. N. Chiu, *J. Phys. Chem. A* **1999**, *103*, 8062–8066; b) Z.-X. Chen, H.-M. Xiao, *Huaxue Xuebao* **1998**, *45*, 1198–1206.

[20] P. N. Gaponik, V. P. Karavai, *Chem. Heterocycl. Compd.* **1984**, 1683–1686.

[21] a) T. M. Klapötke, C. M. Sabate, J. M. Welch, *Z. Anorg. Allg. Chem.* **2008**, *634*, 857–866; b) J. C. Gálvez-Ruiz, G. Holl, K. Karaghiosoff, T. M. Klapötke, K. Löhnwitz, P. Mayer, H. Nöth, K. Polborn, C. J. Rohbogner, M. Suter, J. J. Weigand, *Inorg. Chem.* **2005**, *44*, 4237–4253.

[22] M.-J. Crawford, K. Karaghiosoff, T. M. Klapötke, F. A. Martin, *Inorg. Chem.* **2009**, *48*, 1731–1743.

[23] A. F. Holleman, N. Wiberg, *Lehrbuch der anorganischen Chemie*, 101 st ed., de Gruyter, New York, **1995**.

[24] M. Hesse, H. Meier, B. Zeh, *Spektroskopische Methoden in der Organischen Chemie*, 6 ed., Georg Thieme Verlag, Stuttgart, New York, **2002**.

[25] a) T. H. Dunning, *J. Chem. Phys.* **1989**, *90*, 1007; b) C. Lee, W. Yang, R. G. Parr, *Phys. Rev. B* **1988**, *37*, 785; c) A. D. Becke, *J. Chem. Phys.* **1993**, *98*, 5648.

[26] Gaussian 09W, Version 7.0, M. J. Frisch, G. W. Trucks, H. B. Schlegel, G. E. Scuseria, M. A. Robb, J. R. Cheeseman, G. Scalmani, V. Barone, B. Mennucci, G. A. Petersson, H. Nakatsuji, M. Caricato, X. Li, H. P. Hratchian, A. F. Izmaylov, J. Bloino, G. Zheng, J. L. Sonnenberg, M. Hada, M. Ehara, K. Toyota, R. Fukuda, J. Hasegawa, M. Ishida, T. Nakajima, Y. Honda, O. Kitao, H. Nakai, T. Vreven, J. A. Montgomery, Jr., J. E. Peralta, F. Ogliaro, M. Bearpark, J. J. Heyd, E. Brothers, K. N. Kudin, V. N. Staroverov, R. Kobayashi, J. Normand, K. Raghavachari, A. Rendell, J. C. Burant, S. S. Iyengar, J. Tomasi, M. Cossi, N. Rega, J. M. Millam, M. Klene, J. E. Knox, J. B. Cross, V. Bakken, C. Adamo, J. Jaramillo, R. Gomperts, R. E. Stratmann, O. Yazyev, A. J. Austin, R. Cammi, C. Pomelli, J. W. Ochterski, R. L. Martin, K. Morokuma, V. G. Zakrzewski, G. A. Voth, P. Salvador, J. J. Dannenberg, S. Dapprich, A. D. Daniels, Ö. Farkas, J. B. Foresman, J. V. Ortiz, J. Cioslowski, and D. J. Fox, Gaussian, Inc., Wallingford CT, **2009**.

[27] H. A. Witek, M. Keiji, *J. Comput. Chem.* **2004**, *25*, 1858–1864.

[28] a) A. Dippold, Thomas M. Klapötke, Franz A. Martin, *Z. Anorg. Allg. Chem.* **2011**, *637*, in press; b) T. Altenburg, T. M. Klapötke, A. Penger, J. Stierstorfer, *Z. Anorg. Allg. Chem.* **2010**, *636*, 463–471.

[29] a) J. W. Ochterski, G. A. Petersson, J. A. Montgomery, Jr., *J. Chem. Phys.* **1996**, *104*, 2598; b) J. A. Montgomery, M. J. Frisch, J. W. Ochterski, G. A. Petersson, *J. Chem. Phys.* **2000**, *112*, 6532.

[30] P. J. Lindstrom, W. G. Mallard, NIST Chemistry Webbook, NIST Standard Reference 69, June 2005, National Institute of Standards and Technology, Gaithersburg MD, 20899 (http://webbook.nist.gov).

[31] a) E. F. C. Byrd, B. M. Rice, *J. Phys. Chem. A* **2006**, *110*, 1005–1013; b) L. A. Curtiss, K. Raghavachari, P. C. Redfern, J. A. Pople, *J. Chem. Phys.* **1997**, *106*, 1063–1079; c) B. M. Rice, S. V. Pai, J. Hare, *Combust. Flame* **1999**, *118*, 445–458.

[32] a) F. Trouton, *Philos. Mag. Zeitschrift wurde erst 2003 gerüdet!* **1884**, *18*, 54–57; b) M. S. Westwell, M. S. Searle, D. J. Wales, D. H. Williams, *J. Am. Chem. Soc.* **1995**, *117*, 5013–5015.

[33] Back-calculated from V(TAG⁺Cl⁻) and the molecular volume of the chloride anion taken from Ref. [34]. Volume of the energtic anion has been derived from the TAG⁺ structure; all other volumes have been back-calculated using the corresponding volume of the energetic anion from single-crystal measurements.

[34] a) H. D. B. Jenkins, H. K. Roobottom, J. Passmore, L. Glasser, *Inorg. Chem.* **1999**, *38*, 3609–3620; b) H. D. B. Jenkins, D. Tudela, L. Glasser, *Inorg. Chem.* **2002**, *41*, 2364–2367.

[35] M. Sućeska, EXPLO5.4 program, Zagreb, Croatia, **2010**.

[36] a) M. Suceska, *Propellants Explos. Pyrotech.* **1991**, *16*, 197–202; b) M. Suceska, *Propellants Explos. Pyrotech.* **1999**, *24*, 280–285; c) M. Sućeska, *Mater. Sci. Forum* **2004**, *465–466*, 325–330.

[37] J. Köhler, R. Meyer, *Explosivstoffe, Vol. 9ᵗʰ edition*, Wiley-VCH, Weinheim, **1998**.

[38] NATO standardization agreement (STANAG) on explosives, no. 4489, 1 st ed., Sept. 17, **1999**.

[39] WIWEB-Standardarbeitsanweisung 4–5.1.02, Ermittlung der Explosionsgefährlichkeit, hier: der Schlagempfindlichkeit mit dem Fallhammer, Nov. 08, **2002**.

[40] http://www.bam.de.

[41] NATO standardization agreement (STANAG) on explosives, friction tests, no.4487, 1 st ed., Aug. 22, **2002**.

[42] WIWEB-Standardarbeitsanweisung 4–5.1.03, Ermittlung der Explosionsgefährlichkeit, hier: der Reibempfindlichkeit mit dem Reibeapparat, Nov. 08, **2002**.

[43] NATO standardization agreement (STANAG) on explosives, electrostatic discharge sensitivity tests, no.4490, 1 st ed., Feb. 19, **2001**.

[44] http://www.ozm.cz/en/sensitivity-tests/esd-2008a-small-scale-electrostatic-spark-sensitivity-test/.

[45] CrysAlis CCD, Oxford Diffraction Ltd., Version 1.171.27p5 beta (release 01–04–2005 CrysAlis171.NET).

[46] CrysAlis RED, Oxford Diffraction Ltd., Version 1.171.27p5 beta (release 01–04–2005 CrysAlis171.NET).

[47] A. Altomare, G. Cascarano, C. Giacovazzo, A. Guagliardi, *J. Appl. Crystallogr.* **1993**, *26*, 343–350.

[48] G. M. Sheldrick, SHELXS-97, Crystal Structure Solutuion, Version 97–1; Institut Anorg. Chemie, University of Göttingen, Germany, **1990**.

[49] G. M. Sheldrick, SHELXL-97, Program for the Refinement of Crystal Structures. University of Göttingen, Germany, **1997**.

[50] L. Farrugia, *J. Appl. Crystallogr.* **1999**, *32*, 837–838.

[51] A. L. Spek, Platon, A Multipurpose Crystallographic Tool, Utrecht University, Utrecht, The Netherlands, **1999**.